

TECHNOLOGY UTILIZATION

**CASE FILE  
COPY**

OPTICAL DEVICES: INSTRUMENTATION

A COMPILATION



NATIONAL AERONAUTICS AND SPACE ADMINISTRATION

## Foreword

The National Aeronautics and Space Administration and the Atomic Energy Commission have established a Technology Utilization Program for the rapid dissemination of information on technological developments which have potential utility outside the aerospace and nuclear communities. By encouraging multiple application of the results of its research and development, NASA and AEC earn for the public an increased return on the public investment in aerospace and nuclear R & D programs.

The items compiled herein describe methods, techniques, and devices used to solve a wide variety of problems in the field of optics. They range from magnifiers for special quality control inspections to a sun shield for the radiometer sensor of a celestial navigation system. The compilation is presented in three sections. The first describes various imaging systems and filters; the second deals with optical systems used in photometry, radiometry, and spectrometry; and the third presents optical devices used in manufacturing and quality control.

This compilation is not intended as a complete survey of the field of optics. Rather, a sampling of many diverse activities is presented for the interest of readers unfamiliar with optical technology. At the same time, various designs and applications are described in sufficient detail to interest designers and engineers in many optics-related fields.

Readers particularly interested in optical devices and applications using coherent light (the laser) may be interested in NASA SP-5937 (01), *Optical Devices: Lasers*.

Additional technical information on individual devices and techniques can be requested by circling the appropriate number on the Reader Service Card enclosed in this compilation.

Unless otherwise stated, NASA contemplates no patent action on the Technology described.

We appreciate comment by readers and welcome hearing about the relevance and utility of the information in this compilation.

Ronald J. Phillips, *Director*  
*Technology Utilization Office*  
*National Aeronautics and Space Administration*

NOTICE • This document was prepared under the sponsorship of the National Aeronautics and Space Administration. Neither the United States Government nor any person acting on behalf of the United States Government assumes any liability resulting from the use of the information contained in this document, or warrants that such use will be free from privately owned rights.

---

For sale by the National Technical Information Service, Springfield, Virginia 22151. \$1.00

# Contents

SECTION 1. Optical Image-Forming Devices and Filters	Page
Correction Filters Remove Defects in Optical Images . . . . .	1
PTFE—Aluminum Films Serve as Neutral Density Filters . . . . .	2
Thin Carbon Film Makes Ultraviolet Bandpass Filter . . . . .	2
Acoustically Controlled Optical Filter . . . . .	3
Elimination of Noise in Coherent Light Imaging Systems . . . . .	3
Filter Improves Quality of Digital TV Images . . . . .	3
New Baffle Improves Glare Resistance of Optical Systems . . . . .	4
Antivignetting Beam Deflector . . . . .	4
Grazing-Incidence X-Ray Telescope . . . . .	5
Selective Vignetting of Type-1 X-Ray Telescopes . . . . .	6
Variable Focus Lens: A Concept . . . . .	6
Biplanar-Viewing System Allows Nonplanar Testing in Wind Tunnels . . . . .	7
Binocular Scanning Apparatus . . . . .	8
Aerial-Image Device Enables Diagrams and Animation to be Inserted in Motion Pictures . . . . .	8
Twin Projectors Aid Visualization of Operator's Field of View . . . . .	9
Oculometer for Remote Tracking of Eye Movement . . . . .	10
Fortran Program Aids Design of Optical Systems . . . . .	10
SECTION 2. Photometry, Radiometry, and Spectrometry	
Improved Relay Optics for Cryogenic Spectroradiometer Detectors . . . . .	11
Uniform Response of Photometer Detector Insured by Scanning Technique . . . . .	12
An Absolute Reflectometer . . . . .	12
Honeycomb Shield Eliminates Stray Light from Scanning Mirror . . . . .	13
Special-Purpose Reflectometer Uses Modified Ulbricht Sphere . . . . .	14
Light-Pulse Simulator . . . . .	14
Spectrophotometric Technique Quantitatively Determines NaMBT Inhibitor in Ethylene Glycol-Water Solutions . . . . .	15
Reflectometer Adaptors . . . . .	16
Integrating Sphere Operates at Visible and Infrared Wavelengths . . . . .	17
Miniature King Furnace for Small-Sample Absorption Spectroscopy . . . . .	17
Calibrated-Intensity Lamp . . . . .	18
High-Resolution Spectrometer Reduces Rate-Dependent Errors at High Counting Rates . . . . .	19
High-Resolution Gamma-Ray Spectrometer . . . . .	20
Multichannel Spectroscopy Guide . . . . .	21

SECTION 3. Manufacturing and Quality Control Devices	Page
Portable Spectrometer Monitors Inert-Gas Welding	
Shield . . . . .	22
Stroboscopic Autocollimator . . . . .	23
Coordinate Locator for Printed Circuit Board Holes:	
A Concept . . . . .	23
Precision Alignment Fixture for Producing Photo-Resist	
Etched Wafers . . . . .	24
Form Gage for Conical Optical Surface . . . . .	24
Magnifier for In-Place Inspection of Tube Flares . . . . .	25
Optical Template Measures Very Small Corner Radii . . . . .	26
Camera System for Printed Circuit Board Inspection . . . . .	26
Device Visually Portrays Semiconductor Surfaces . . . . .	26
Improved Optical Probe for Combustion Chambers . . . . .	27

# Section 1. Optical Image-Forming Devices and Filters

## CORRECTION FILTERS REMOVE DEFECTS IN OPTICAL IMAGES

Four theoretically derived filters can correct photographic image deficiencies caused by defocusing, lateral shift with double exposure, ring smear, and linear smear. The complete derivations of the four compensating filters are presented in supporting documentation. For the purposes of illustration, only the first derivation, for the filter which corrects defocusing, is outlined here.

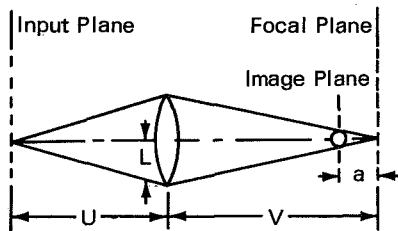


Figure 1. System Response to Unsharp Focusing

Figure 1 illustrates the characteristic behavior of a defocused optical system: A circular image of finite radius is produced from a point source of illumination.

The point source is defined as

$$b(x,y) = B_0 \delta(x,y),$$

where  $b(x,y)$  is the energy distribution of the source,

$B_0$  is the source intensity, in lumens, and

$$\delta(x,y) = \begin{cases} 1 & \text{at } x^2 + y^2 = 0 \\ 0 & \text{for all } x^2 + y^2 \neq 0. \end{cases}$$

Assuming that the blurred image has a uniform intensity distribution and that the optical system is lossless, the image can be described as

$$p(x,y) = \begin{cases} \frac{B_0}{a^2} \left(\frac{V}{U}\right)^2 & \text{for } x^2 + y^2 \leq r_0^2 \\ 0 & \text{for } x^2 + y^2 > r_0^2 \end{cases}$$

where  $p(x,y)$  is the energy distribution of the image, and  $U$ ,  $V$ , and  $a$  are the object, image,

and defocal distances, respectively, defined in Figure.1.

The normalized modulation transfer function (Fourier transform) from  $b(x,y)$  to  $p(x,y)$  is

$$H(\rho) = \frac{2 J_1(2\pi\rho r_0)}{2\pi\rho r_0}$$

where  $H(\rho)$  is the transfer function,  $J_1$  is the Bessel function of the first order,

$$\rho = (\omega_x^2 + \omega_y^2)^{1/2},$$

and  $\omega_x, \omega_y$  are Fourier-transformed polar coordinates.

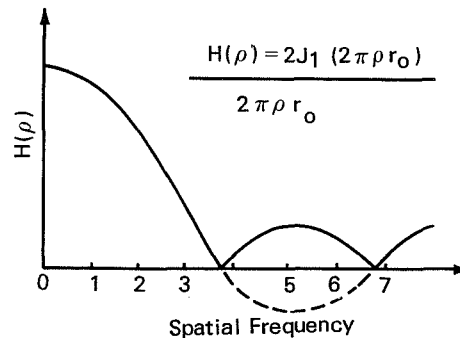


Figure 2. Transfer Function of the Unsharp Focus Response to a Point Source

The plot of this function is shown in Figure 2. Note that, with coherent light, the transfer function goes negative, whereas with normal, incoherent light, the phase information is lost and only the intensity data is detectable.

The modulation transfer function shows the characteristics of a low pass filter. High spatial-frequency data (fine details of the image) are attenuated.

It seems obvious, and is in fact the case, that the modulation transfer function  $F(\rho)$  of the compensating filter that can restore the image to a more faithful reproduction of the scene, is just the reciprocal of  $H(\rho)$ .

A correction filter that approximately duplicates  $F(\rho)$  can be produced by simultaneously scanning the defocused image with two color-coded detectors in the form of a uniform red aperture with a blue pinhole in the center. By subtracting the signals from the red and blue detectors, a resultant light intensity is produced which closely approximates  $F(\rho)$  up to some maximum spatial frequency determined by the aperture size. It should be noted that the compensation is performed point by point during the scanning

process, and that the filter is tuneable. The optimum compensation for a blurred image will be obtained when the radii of the red circle and the blur circle are equal.

Source: S. Y. Lee of  
Bellcomm, Inc.  
under contract to  
NASA Headquarters  
(HQN-10542)

*Circle 1 on Reader Service Card.*

### PTFE—ALUMINUM FILMS SERVE AS NEUTRAL DENSITY FILTERS

A series of neutral-density, broad-band filters in the wavelength range 0.3 to 2.1  $\mu\text{m}$  can be made by vapor-depositing aluminum on polytetrafluoroethylene (PTFE) films. The filters, useful for calibrating, are formed using a 25.4  $\mu\text{m}$  (1 mil) thick PTFE film, which has an optical density of approximately 0.03 at a wavelength of 1  $\mu\text{m}$ . Aluminum may be vapor deposited on the film surface in thicknesses up to 0.011  $\mu\text{m}$ .

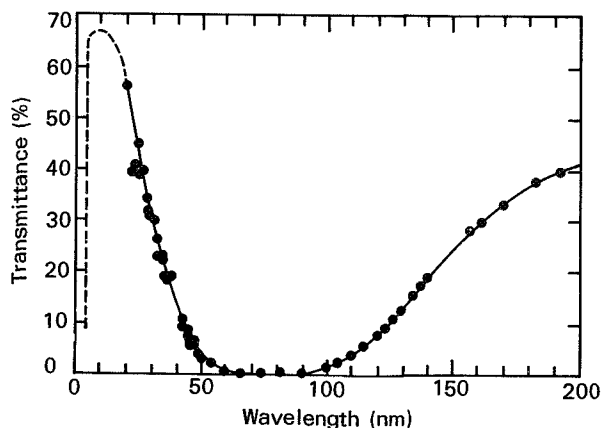
At the maximum thickness, the resulting filter has an optical density of approximately 1.30 at the 1  $\mu\text{m}$  wavelength. The optical density may be varied between these two limits by controlling the thickness of the aluminum deposit.

Source: H. D. Burks of  
Langley Research Center  
(LAR-00189)

*Circle 2 on Reader Service Card.*

### THIN CARBON FILM MAKES ULTRAVIOLET BANDPASS FILTER

Another thin-film filter suppresses undesired wavelengths for narrow-band, far-ultraviolet detectors that operate at wavelengths shorter than



the lithium fluoride cutoff. The filter also suppresses scattered light and lines of unwanted orders in vacuum spectrographs.

The filter consists of a 27 nm thick carbon film, evaporated onto a glass slide, floated off in water, and picked up on a 70% transparent gold-mesh screen. The filter has an average transmittance of 47% for the visible light emitted from a tungsten lamp.

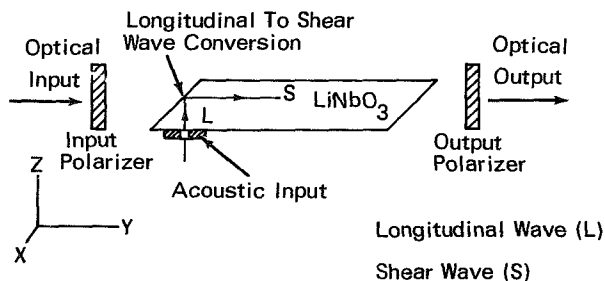
The figure shows the filter characteristics in the far ultraviolet. The transmittance decreases smoothly from 41% at 200 nm to 1% at 100 nm. Between 90 and 60 nm, the film is highly absorbent. In the vicinity of the free-electron plasma wavelength (52.6 nm) the transmittance begins to increase, reaching 56% at 20.9 nm. Presumably, the transmittance will reach a maximum at shorter wavelengths before falling to zero at the carbon K absorption edge, 4.36 nm.

Source: GCA Corp.  
under contract to  
NASA Headquarters  
(ERC-00008)

*Circle 3 on Reader Service Card.*

## ACOUSTICALLY CONTROLLED OPTICAL FILTER

A completely different kind of filter is represented by a recently conceived, narrow band optical filter that is electronically tuneable over a wide wavelength band. Basically, the filter



operates by colinear acousto-optic diffraction in an anisotropic medium. One of several possible configurations for the filter is illustrated, using a lithium niobate crystal. A longitudinal acoustic wave is introduced near one end and converted to a shear wave upon internal reflection from the (optical) input face of the crystal. The acoustic shear wave and the optical beam then propagate colinearly down the y-axis of the

crystal, allowing the acousto-optic interaction to occur.

Such a filter should be tuneable over the entire visible wavelength band (400-700 nm) by supplying an acoustic wave in the frequency band from 423 MHz to 990 MHz. The angular aperture will be about 0.024 rad, and it should be possible to attain nearly 100% transmission at the filter's center frequency with an expenditure of about 14 mW of acoustic power per mm<sup>2</sup> of filter aperture.

Title to this invention has been waived under the provisions of the National Aeronautics and Space Act [42 U.S.C. 2457 (f)], to the Stanford University, Stanford, California 94305.

Source: S. E. Harris of  
Stanford University  
under contract to  
Headquarters  
(HQN-10440)

*No further documentation is available.*

## ELIMINATION OF NOISE IN COHERENT LIGHT IMAGING SYSTEMS

Minor defects in the components of optical systems using coherent light cause objectionable bull's-eye diffraction patterns to appear in the image. Dust particles and bubbles both in and on lenses are largely responsible. The patterns can be eliminated by simply rotating the lens about its optical axis. By this technique, the diffracted energy, normally concentrated over a very small area of the image, is spread over a much

larger annular area. Unless the defect causing the diffraction lies very close to the optical axis, the diffracted energy is averaged out and can be ignored. Note that the technique has no effect on the spatial coherence of the light.

Source: A. R. Shulman et.al.,  
Goddard Space Flight Center  
(GSC-11133)

*Circle 4 on Reader Service Card.*

## FILTER IMPROVES QUALITY OF DIGITAL TV IMAGES

An optical filter for modulating a picture scene with pseudo-random noise, prior to its conversion into an electrical signal for transmission over a narrow-band video channel, can reduce the appearance of quantizing contours when the scene is reconstructed. The pseudo-random noise pattern is developed on a variable-density filter, which is placed over the input lens of the TV camera tube. As a result, the video signal output from the tube is the product of both the noise pattern and the image supplied to the tube. At the receiving station, a complementary filter may be used to remove the noise pattern from

the output, to yield an image of greater overall quality than would be possible without the filter.

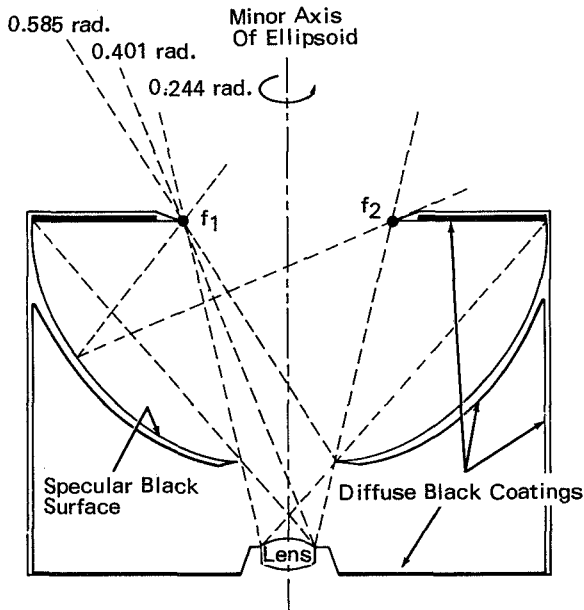
In specialized digital TV systems currently in existence, a similar effect is normally gained through introduction of pseudo-random electrical noise. The optical technique described here is much simpler and less expensive.

Source: C. J. Byrne of  
Bellcomm, Inc.  
under contract to  
NASA Headquarters  
(HQN-09985)

*Circle 5 on Reader Service Card.*

### NEW BAFFLE IMPROVES GLARE RESISTANCE OF OPTICAL SYSTEMS

The baffle configuration shown in the illustration provides a more efficient shade against interfering sources of illumination outside the desired field of view of optical imaging systems.



This baffle consists of a semi-ellipsoid of revolution about the minor axis, coated with a black, specular reflecting surface, and an aperture defined by the locus of the foci ( $f_1$ ,  $f_2$ ) of the generating ellipse. The baffle works because of the familiar property of a planar ellipse, that any incoming ray that intersects one focus will

intersect the other focus after reflection from the ellipse. In the case of this ellipsoid, a locus of foci exists in the form of a circle normal to the axis of revolution. Any incoming ray that intersects this locus will, after reflection, intersect the locus again, at a diametrically opposite point. Therefore, the geometry and specular reflecting surface make a virtually perfect internal baffle for stray light. None of the light entering the baffle is trapped inside.

The illustration represents a cross-section of a shade for a lens with a conical field of view of 0.244 rad half angle. The foci  $f_1$  and  $f_2$ , in each elliptical section, lie on the rays defining the clear field of view of the optical system. The major axis of the ellipsoid is chosen so that the surface which is directly illuminated with stray light is not visible from the lens. The shading properties of this ellipsoid configuration are effective for all stray light emanating from angles greater than 0.585 rad. All shade surfaces that are visible from the lens are given a diffuse black coating to prevent interference from internally diffused light.

Source: E. S. Davis of  
Caltech/JPL  
under contract to  
NASA Pasadena Office  
(NPO-10337)

*Circle 5 on Reader Service Card*

### ANTIVIGNETTING BEAM DEFLECTOR

It is sometimes necessary to introduce into a beam of light a small but precise deflection with respect either to the optical axis of a telescope or to another beam that is being collected or expanded by the same telescope. An example of this requirement is given by laser tracking telescopes, where transit time and the aberration of light introduce the need for an offset between transmitted and received lines of sight. When the beam to be offset is a received beam, the situation is not severe, because the aperture of the optics can be increased to accept the wide field without vignetting. To offset a transmitted beam, however, is more difficult, because the optical

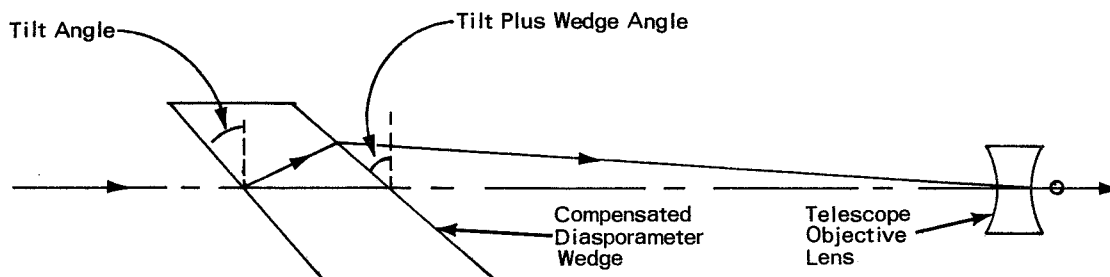
components involved include the main telescope, which is generally the limiting element in the system.

One existing means of rendering a deviated beam coincident with a desired path is the use of an aperture-transfer telescope. This device consists of two identical lenses whose focal lengths are approximately one fourth of the distance between the beam-bending element and the telescope eyepiece. One lens forms a real image of the transmitter and the other recollimates the beam. During operation, the phase of the bending element is inverted so that the sense will be correct after the action of the telescope.



The disadvantage of this approach is that it requires the use of additional optical elements within a comparatively long path length free of other elements.

A third method of compensating is to place the diasporameter in the tracking line of sight, which will cause the tracker to offset and leave the transmitter on axis. This requires enlarging



The new technique for accomplishing the same function, without additional optics or added length, is the compensated diasporameter illustrated in the figure. Each wedge of the diasporameter is made with a finite thickness and is installed at the proper tilt angle to translate the line of sight in a sense opposite the deviation angle. The thickness and tilt angle are calculated to cause the emerging beam to cross the axis at the desired point.

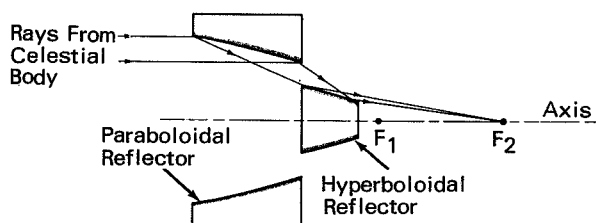
the acceptance field of the tracker optics, which in some cases may not be practical.

Source: W. P. Devereux of  
Kollsman Instrument Corp.  
under contract to  
Marshall Space Flight Center  
(MFS-14419)

Circle 6 on Reader Service Card.

### GRAZING-INCIDENCE X-RAY TELESCOPE

A grazing-incidence telescope may be used for observing distant celestial bodies at wavelengths between 0.3 and 50 nm.



In addition, the device can be used as a fore-optics system for an extreme-ultraviolet spectrometer, or for the collection or "imaging" of thermal neutrons. Conventional optical systems either do not operate efficiently over portions of this wavelength region, are too large, or cannot be conveniently matched to a spectrometer.

As shown in the illustration, the telescope is essentially a glancing-incidence Cassegrain reflector system composed of a concave paraboloid of revolution followed by a convex hyperboloid of revolution. The two reflectors are mounted such that they are confocal at  $F_1$ . Incident rays which are parallel to the axis of the system tend to converge toward  $F_1$ . These rays are reflected by the convex hyperboloid to  $F_2$ , the conjugate focus of the hyperboloid. The image at this focus may be cast onto a photographic plate or upon the entrance slit of another optical instrument, such as a glancing-incidence or Bragg crystal spectrometer.

Source: W. M. Neupert and J. H. Underwood  
Goddard Space Flight Center  
(GSC-10052)

Circle 7 on Reader Service Card.

### SELECTIVE VIGNETTING OF TYPE-1 X-RAY TELESCOPES

A new technique optimizes the performance of a Type-1 (concave parabola followed by a concave hyperbola) X-ray telescope by applying a special ray-tracing program. The image quality of the telescope system is improved by matching the detector to the optimum focal surface and by vignetting rays which formerly contributed to the flare in comatic images.

Analysis of the optical imaging characteristics of the Type-1 X-ray telescope permits the quantitative design of experiments using such optics, with full understanding of the trade-off in spectral resolving power versus weight and optical efficiency.

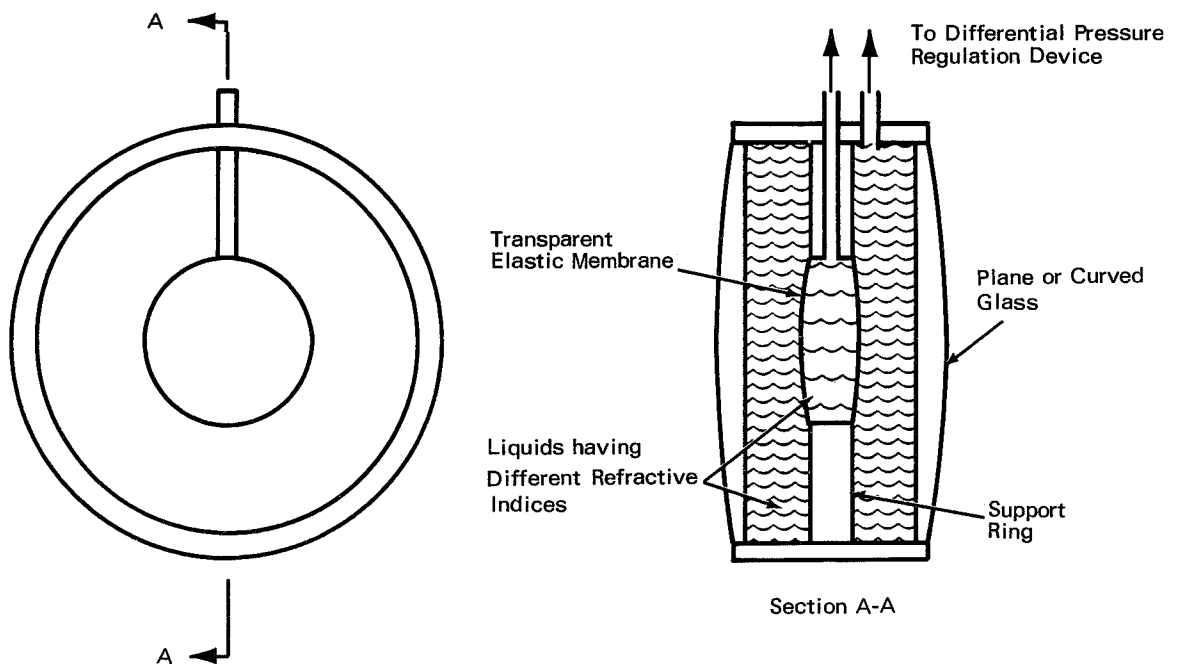
Vignetting, of itself, is not new in this type of telescope, but the "selective" vignetting technique involved here is the first quantitative technique with the following advantages: (1)

image quality is enhanced (or spatial resolving power is increased) by decreasing the length of the secondary (hyperbolic) element of the telescope. (2) An optimization point in the foreshortening of the hyperbolic element is established. Beyond this point, if the element length is further decreased, loss of energy in the image results, without a compensating improvement in image quality. (3) The minimal area requiring optical figuring is established. (4) Telescope weight and size are decreased to a minimum while an optical resolving power exceeding that of the unvignetted configuration is attained.

Source: J. Mangus  
Goddard Space Flight Center  
(GSC-10682)

Circle 8 on Reader Service Card.

### VARIABLE FOCUS LENS: A CONCEPT



Focus adjustment in optical instruments is almost universally accomplished by changing the axial distances between the elements of the instrument. However, in some applications, adjust-

ing the lens curvature, a mechanism similar to that employed by vertebrate eyes, may be a more desirable technique. A possible approach is shown in the figure. The lens is a lenticular

pod of plastic containing a clear liquid or gel of relatively high refractive index. The pod is supported in a transparent container filled with a liquid or gel of lower refractive index but similar density. Lens curvature may then be controlled by changing the relative pressure in the two liquids.

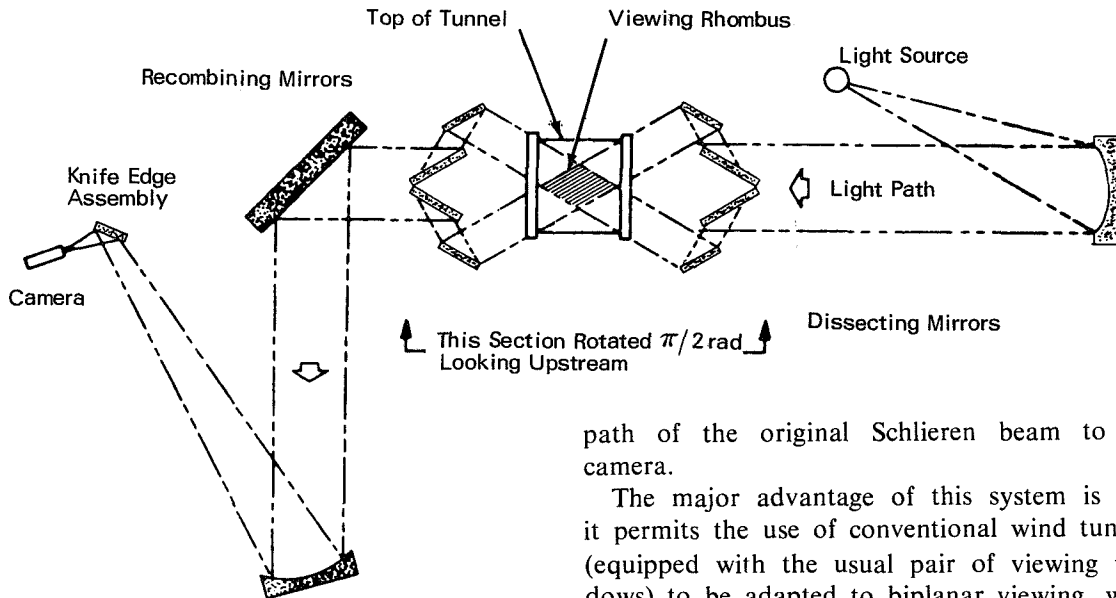
Source: J. Howe of Allied Research Associates, Inc. under contract to NASA Headquarters (HQN-10408)

*No further documentation is available.*

### BIPLANAR-VIEWING SYSTEM ALLOWS NONPLANAR TESTING IN WIND TUNNELS

A wind tunnel Schlieren optical system has been modified to incorporate a biplanar viewing system, allowing an aerodynamic model to be observed from two angles, while permitting both

within which a model trajectory can be observed in two planes. At the output viewing window, a symmetrical set of mirrors recombines the beam and directs the two images along the



views to be recorded simultaneously with a single, original camera. As shown in the figure, a set of four front-surfaced mirrors is positioned within an existing Schlieren light beam. The mirrors are adjusted to split the beam into two parts, which are directed through the test section at angles of approximately  $\pi/6$  rad ( $30^\circ$ ) above and below the horizontal. A viewing rhombus is created in the wind tunnel test section.

path of the original Schlieren beam to the camera.

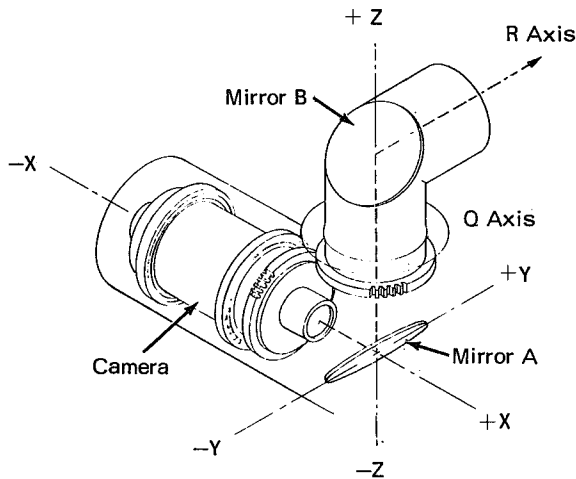
The major advantage of this system is that it permits the use of conventional wind tunnels (equipped with the usual pair of viewing windows) to be adapted to biplanar viewing, without the extensive alterations that would be needed, for instance, to modify the facility for a pair of windows orthogonal to the first.

Source: H. P. Holway of Caltech/JPL under contract to NASA Pasadena Office (XNP-9829)

*Circle 9 on Reader Service Card.*

### BINOCULAR SCANNING APPARATUS

An optical gimbaling apparatus can direct a narrow field of view through a solid angle approaching  $4\pi$  steradians. It minimizes size, weight, and power when large instruments are required, and provides the basis for a binocular scanning capability. Image rotation produced by



scanning can be altered (or eliminated) as desired by gear trains directly linked to the scanning apparatus.

The figure shows a camera aligned along the +X axis to record the image reflected from mirror A of the scanning apparatus. Scanning may be accomplished by rotating mirror B about the Q axis. As this is done, however, the orientation of the image seen by the camera also rotates. When the viewing direction (the R axis) points

in the +X direction, the image is upright. As mirror B rotates, the image rolls over at such a rate that, when the R axis points in the -X direction, the image is upside down. The gear trains are designed to rotate the camera at the same rate, so that it will record an upright picture regardless of the orientation of the R axis.

Scanning may also be accomplished by rotating mirrors A and B (fixed with respect to each other) about the X axis. This technique produces a different sort of image rotation. In either case, directly linked gear trains utilizing differentials can be employed to obtain the image orientation desired.

A more elaborate configuration permits binocular information to be extracted without the use of slaved gimbal systems. A minimum separation of axes maximizes the available field of view and reduces packaging volume, while the extension of cross-arms carrying mirrors increases the boresight offset for a greater binocular effect. In the latter case, if an illuminator is used in one side, an increased geometric isolation from near-field-particle or Raleigh-scattering phenomena is achieved.

Source: G. L. Parker and F. R. Chamberlain of  
Jet Propulsion Laboratory  
under contract to  
NASA Pasadena Office  
(NPO-11002)

*Circle 10 on Reader Service Card.*

### AERIAL-IMAGE DEVICE ENABLES DIAGRAMS AND ANIMATION TO BE INSERTED IN MOTION PICTURES

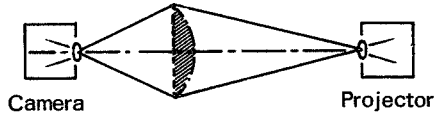
In technical motion picture production, it is often desirable to show the internal construction of complicated machinery, or to insert diagrams and animation into live pictures. It is also sometimes helpful if the general details of a picture can be suppressed, thus outlining or "lifting" an element from a confusing background.

An aerial-image unit makes it possible to insert diagrams and animation into live pictures, and also to lift an element from a confusing background by suppressing general details. The unit consists of a projector which illuminates

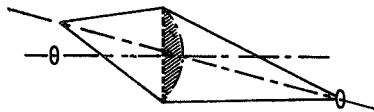
the field lens of an animation stand. This lens deflects the projected image to a camera. Cell material (artwork prepared on transparent sheets of film) can be laid over the field lens to mask the image. The use of high-quality camera and projector lenses, and critical alignment of the system, are essential to making the system effective.

The aerial-image unit, shown in illustration A, includes a combination of two separate lens systems: the camera-projector system and the field lens system. The projector focuses a real image

on the field lens, and the image is rephotographed by the camera. The projection and camera lenses must operate near maximum aperture; therefore, very high quality lenses are required



A) Field Lens System  
Aerial Image Optics



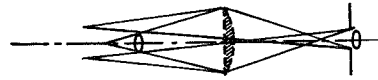
B) System Misaligned (camera does not "see" projector lens).

in order to avoid loss of definition. Critical alignment is essential, for if the image does not fall directly on the camera lens, the camera will not "see" the picture (illustration B).

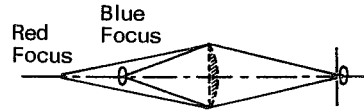
Illustrations C and D show the effects of chromatic aberration, which can cause color fringes to appear around the image. In C, this problem has been eliminated by using a large

aperture projector together with a small aperture camera.

In D, use of a small aperture projector has multiplied the aberration to such an extent that



C) Chromatic Aberration; Large Aperture Projector (camera does not "see" color fringe).



D) Small Aperture Projector (image will appear blue).

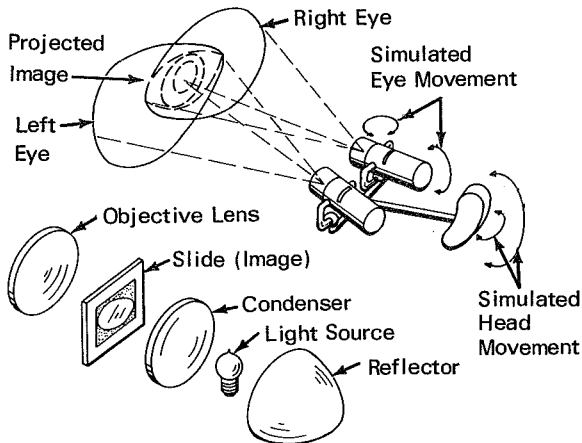
the color tone of the whole image is affected. The color that is emphasized depends on the exact location of the camera lens. This aberration may thus be applied for special effects.

Source: G. W. Tressel and S. J. Andrews, Jr.  
Argonne National Laboratory  
(ARG-00165)

*No further documentation is available.*

### TWIN PROJECTORS AID VISUALIZATION OF OPERATOR'S FIELD OF VIEW

The device shown in the illustration is used in the planning and layout of control panels. It projects a pattern corresponding to the limits



of an operator's vision in any direction he may be required to look, and it aids evaluation of visual ability at any point on the panel.

The device consists of two projectors that can

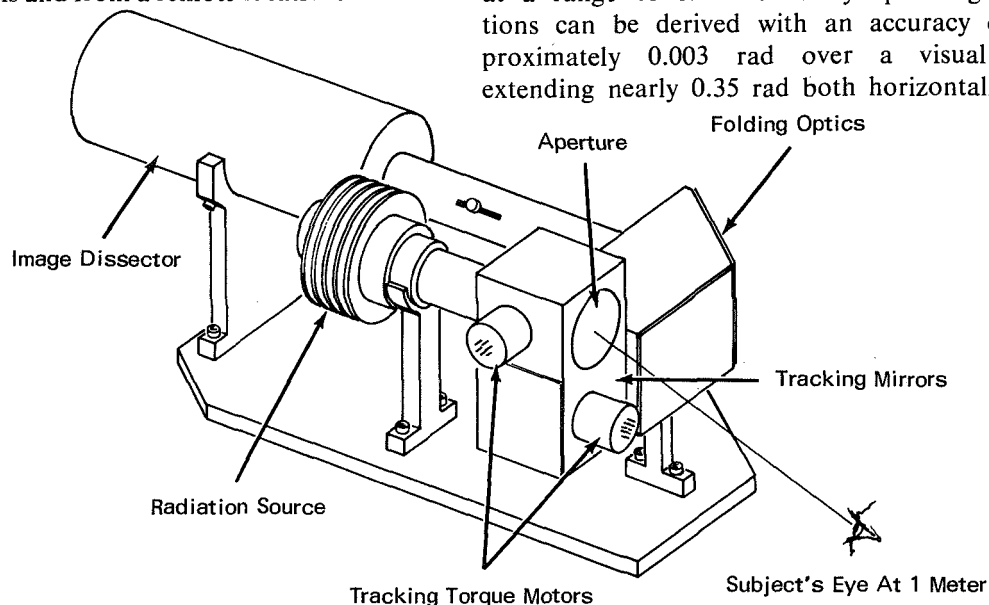
be pivoted to simulate the range of movement of the human eye and head. Each projector contains a reflector, a light source, a filter, a slide containing an image, and an objective lens. The light is reflected to the filter, where it is diffused to uniformly illuminate the image-containing visual pattern slide and to project the image by means of the objective lens. The two images converge at a focal point in a binocular projection, determined by the simulated eye and head movements. The projected image reveals areas on the panel that are blind to either or both eyes, due to framework, supports, handles, etc., located between the panel and the operator.

Source: R. A. Beam of  
North American Rockwell, Inc.  
under contract to  
NASA Pasadena Office  
(WOO-00250)

*No further documentation is available.*

### OCULOMETER FOR REMOTE TRACKING OF EYE MOVEMENT

The illustrated prototype oculometer tracks lateral eye position and measures the direction of the eye's optical axis, pupil size, and blink frequency. It can perform measurements on a real-time basis and from a remote location.



In operation, the eye is irradiated by a collimated beam of near-infrared energy. The beam continuously tracks eye position by means of two orthogonal, servo-controlled mirrors. An electro-optic image dissector detects the near-infrared energy reflected from the eye's corneal and retinal surfaces. Data on corneal-reflection positions relative to the centroid of the pupil-iris

boundary, eye pointing directions, and other eye movements are electronically derived from the detected signal. The prototype instrument will accommodate lateral eye displacements of 12 cm at a range of one meter. Eye pointing directions can be derived with an accuracy of approximately 0.003 rad over a visual field extending nearly 0.35 rad both horizontally and

vertically. The measurement of pupil diameter is substantially linear from 2 to 9 mm.  
Source: J. Merchant and K. A. Mason of Honeywell, Inc. under contract to Electronics Research Center (ERC-10114)

*Circle 11 on Reader Service Card.*

### FORTRAN PROGRAM AIDS DESIGN OF OPTICAL SYSTEMS

A computer has been programmed to use the principles of geometrical optics to design and/or evaluate optical systems containing up to 100 planes, conic or polynomial aspheric surfaces, 7 object points, 6 colors, and 200 rays.

The program, written in Fortran IV for use on an IBM 7094 computer equipped with an SC-4020 plotter, is made up of 48 subroutines. It uses iteration combined with a linear least-squares minimization technique to reduce the magnitude of the merit function by automatically adjusting system parameters. (The merit function

is the length of the error vector whose components are the weighted deviations from the mean of ray coordinates at the image.)

Among the user-selected options are: design computation, spot-diagram computation, twin-ray diagnostic for maximum-size object, twin-ray diagnostic for a zero object, and sensitivity computations. The user can also choose the weighting factors which are combined with spot size to make up the merit function. These factors govern: (1) focal length deviation; (2) exit pupil deviation; (3) spot size for each object point;

(4) spot size for each specified color; (5) spot diagram size in the X-direction; (6) spot diagram size in the Y-direction; (7) lateral chromatic aberration for each object point; and (8) image height deviations for each object point.

The individual rays of the specified pattern are traced from the object points through the lens system to a point on the image plane by using a three-step iterative procedure. The coordinates of each ray on each surface, and the direction of each ray following refraction (which here includes reflection as a special case), are found at each surface from the coordinates and

direction of the ray at the preceding surface. Focal point, focal length, back focus, f-number, and exit pupil location are found for every color. The output resulting from an initial ray pattern can be plotted.

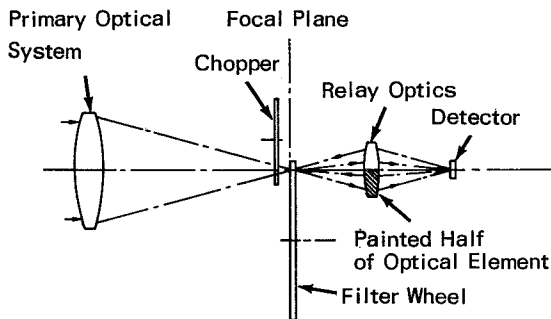
Source: L. F. Schmidt of  
Jet Propulsion Laboratory, with  
P. J. Firnett and L. A. Wilson of  
Informatics, Inc.  
under contract to  
NASA Pasadena Office  
(NPO-10603)

*Circle 12 on Reader Service Card.*

## Section 2. Photometry, Radiometry, and Spectrometry

### IMPROVED RELAY OPTICS FOR CRYOGENIC SPECTRORADIOMETER DETECTORS

In a spectroradiometer using a variable filter wheel, relay optics are generally needed to re-image radiation passing through the filter onto a cryogenically cooled detector. The radiation



reaching the detector consists of the chopped radiation passing through the filter wheel, the radiation emitted by the detector itself and reflected by the filter, and the radiation emitted by the filter and the relay optics. However, the reflectivity of the back of the filter wheel is not constant, but varies in an irregular manner with the spectral passband.

The effect of radiation reflected from the back of the filter wheel can be eliminated optically by coating half of one element in the relay optical system with a very high emissivity paint. This causes the detector to view a constant level

of radiation, regardless of how the reflectivity of the back of the filter wheel changes. As the wheel rotates, its reflectivity changes, the amount of radiation emitted by the blackened half of the relay optics, reflected off the back of the filter wheel, and focused onto the detector also changes, in direct proportion. Since the reflectivity and emissivity must add to unity in all spectral bands (except the very narrow passband of the wheel), the change in radiation reflected by the filter wheel is balanced by the change in radiation emitted by the wheel itself. Therefore, if the filter wheel and the relay optics are at the same ambient temperature, the radiation reaching the detector appears as though it were emitted by a constant source at ambient temperature. Since this radiation is constant with time, it can be separated electronically from the chopped radiation passing through the filter wheel merely by using an ac-coupled preamplifier.

Source: A. R. Kraemer of  
Lockheed Missiles and Space Co.  
under contract to  
Manned Spacecraft Center  
(MSC-11688)

*No further documentation is available.*

### UNIFORM RESPONSE OF PHOTOMETER DETECTOR INSURED BY SCANNING TECHNIQUE

The transmittance and reflectance measuring method recently developed can effectively achieve uniform detector response without accepting the efficiency and bandwidth limitations imposed by such devices as diffusing screens and integrating spheres. In measuring transmittance and re-

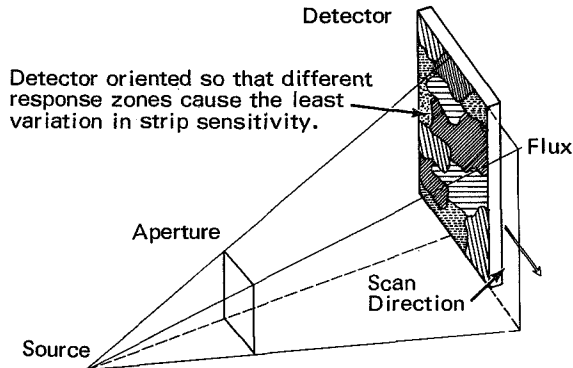


Figure 1. Schematic Representation of the Scanning Process.

fectance of rough-surfaced materials, the detector must be impartial with respect to the distribution of the intercepted radiant flux. Yet, polycrystalline and large-area single-crystal detectors commonly show large variations in sensitivity from point to point on their surfaces.

The central concept behind the new technique is that local detector response and variation in intercepted radiant flux are two independent, random variables. This being the case, a simple scanning process, in which each flux element is successively paired with all the detector elements lying along a given strip, can be used to eliminate the detector's response variation.

The implementation steps involved are as follows: First, the sensitivity variation of the detector is measured, and a map is prepared showing

the sensitivity contours on the detector face. Second, the detector is mounted in a travelling carriage, as shown in Figure 1, and oriented so as to minimize the fluctuations about the mean

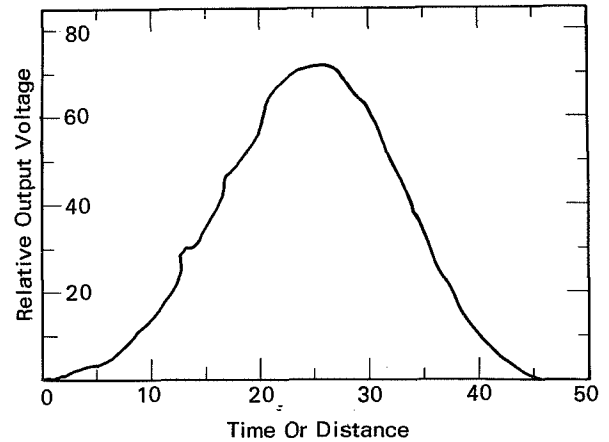


Figure 2. Typical Response Curve of the Scanning Process.

sensitivity for all strips. Finally, using a  $\pi$  rad ( $180^\circ$ ) ellipsoidal collector and a scan rate of about 0.2 cm/min, a response curve is plotted. (A typical response curve is shown in Figure 2.) The area under the response curve is then integrated with a planimeter to derive the total reflectance/transmittance data.

Measurements made on standard samples with and without scanning have been compared to measurements made with an integrating sphere. On repeated measurements, a 12% error for the non-scanning technique was fairly consistently reduced to about 4% by the use of scanning.

Source: M. W. Finkel  
Goddard Space Flight Center  
(GSC-10739)

Circle 13 on Reader Service Card.

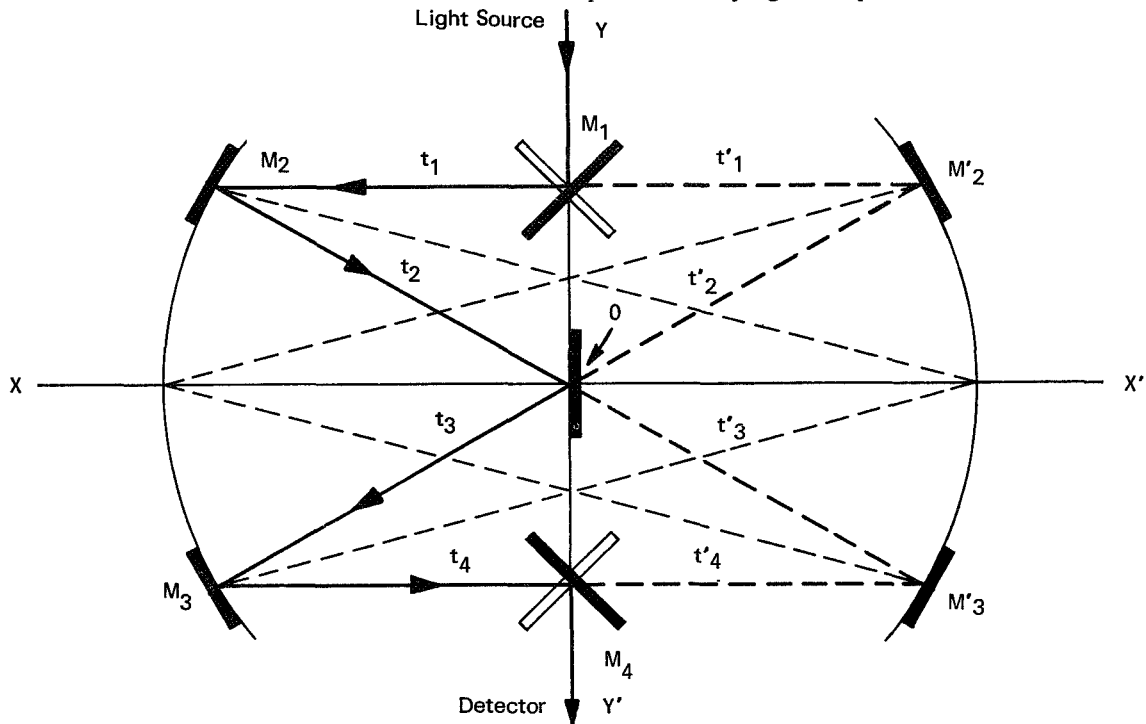
### AN ABSOLUTE REFLECTOMETER

A Czerny-Turner optical system incorporating a novel array of plane and spherical mirrors can collimate an incident light beam onto a sample surface and then direct the reflected light beam onto a photodetector. The arrangement of the array diagrammed in the illustration permits the incident beam to reach the detector via any one

of four routes. With the sample in position at 0 and the two plane mirrors,  $M_1$  and  $M_4$ , in the shaded positions shown, the incident light is directed from  $M_1$  to  $M_2$  (where it is collimated) to the surface, and the reflected beam reaches the detector via  $M_3$  and  $M_4$ . With the specimen removed and mirror  $M_4$  rotated to its



alternate position, the incident beam is reflected from  $M_2$  to  $M'_3$  to  $M_4$  and the detector. Two other symmetrical paths exist with mirror  $M_1$  in its alternate position and the orientation of the sample reversed.



device is absolute.) Further, the measurements can be made using white or monochromatic light, plane or circularly polarized, over a wide range of wavelengths. A simple scissors mechanism permits varying the positions of the mirrors

The absolute reflectance of a sample surface can be computed from these two pairs of measurements independently of any absorption or scattering anywhere within the system. The optical system is automatically corrected for all aberrations except astigmatism and field curvature, both of which can be made negligible by using proper entrance and exit slits or by restricting the field of view.

The purpose of this new design is to measure the specular reflectance of a plane surface without comparison to any standard surface. (The

simultaneously, allowing measurements to be made over a wide range of angles of incidence. A simple modification involving three calibrated plane mirrors allows the reflectometer to be used with samples of arbitrarily large size.

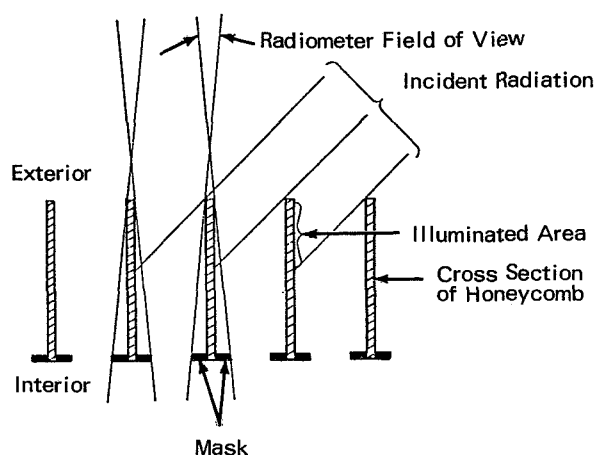
Source: R. Beer of  
Caltech/JPL  
under contract to  
NASA Pasadena Office  
(NPO-10794)

*Circle 14 on Reader Service Card.*

### HONEYCOMB SHIELD ELIMINATES STRAY LIGHT FROM SCANNING MIRROR

A modified honeycomb structure is used to shield the scanning mirror of a high-performance radiometer. The mirror must be shielded from direct illumination by the sun in order to prevent

production of excessive signals and possible damage to the instrument. However, it is impractical to use a standard sunshade big enough to fit the large aperture of the radiometer.



The modified honeycomb structure (shown in cross section) is placed in the aperture of the radiometer in front of the scanning mirror. The honeycomb limits the view angle (away from the scan axis) from which light can fall directly on the mirror surface. The baffle plate behind the honeycomb masks the mirror from light reflected by the honeycomb structure.

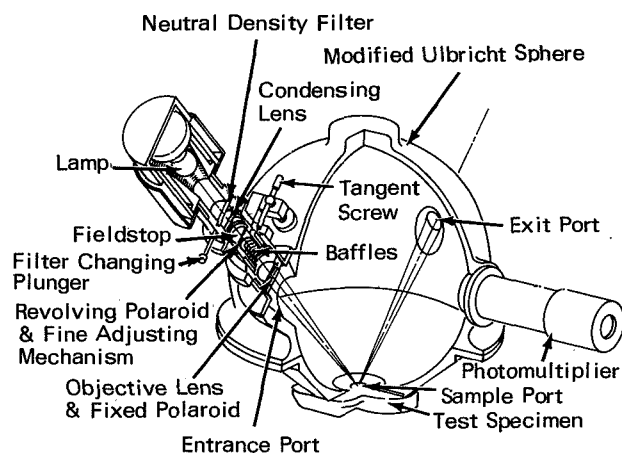
Source: J. E. Armington of Radio Corporation of America under contract to Goddard Space Flight Center (GSC-10676)

Circle 15 on Reader Service Card.

### SPECIAL-PURPOSE REFLECTOMETER USES MODIFIED ULBRICHT SPHERE

An instrument has been devised that will accurately measure the degree by which an optical surface departs from the ideal. Surface

ubiquitous solar radiation. Therefore, rigid requirements are imposed on the surfaces of mirrors or prisms used in navigation instruments.



As illustrated, the instrument is essentially a modified Ulbricht sphere that accurately measures all stray radiation caused by irregularities in the reflective surface of an optical test specimen. The test specimen is so positioned between a light source and exit port that, in the case of an ideal surface, the interior wall of the sphere would remain dark. In the case of an actual test specimen, all diffusely scattered radiation is collected and averaged by the reflectively treated inner wall of the sphere, then measured by a photomultiplier tube attached to a port in the sphere wall.

Source: Mark Gorstein of Massachusetts Institute of Technology under contract to Manned Spacecraft Center (MSC-01135)

imperfections that are normally acceptable become intolerable sources of stray solar radiation in space navigation applications involving seeking and identifying spectral bodies in the presence of

Circle 16 on Reader Service Card.

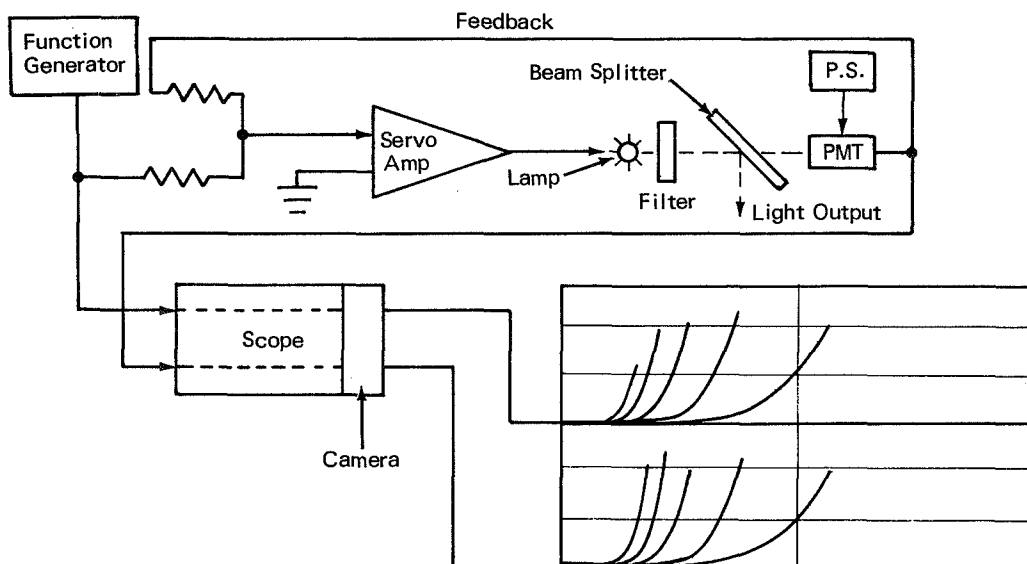
### LIGHT-PULSE SIMULATOR

A light source has been devised that simulates an exponential light energy distribution. It is intended for use in calibrating a light analyzer

that measures light energy from meteor trails. Such an analyzer should be capable of recording both the peak intensity of the light and the

range of intensities leading up to the peak. The difficulty of achieving this dual capability, while maintaining accurate calibration, is compounded if the light analyzer is extremely sensitive.

signal and fed through a servo amplifier to the tungsten-filament lamp. The lamp output is split: part goes to the instrument being calibrated, and part goes to a photomultiplier tube. The



In the new technique, a conventional feedback system using an electro-optical servo causes the calibration lamp to change in intensity according to the time dependent function  $V = V_0 e^{at}$ . This source can be used to establish and maintain accurate calibration of the instrument with respect to both the intensity range and the peak intensity.

As shown in the diagram, an exponential waveform is input to the system as an electrical

output of the photomultiplier is fed back to the servo amplifier to control the lamp current.

Source: C. D. Bass, F. N. Mastrup, and R. Yamasaki of Thompson Ramo Woolridge under contract to Manned Spacecraft Center (MSC-13154)

Circle 17 on Reader Service Card.

### SPECTROPHOTOMETRIC TECHNIQUE QUANTITATIVELY DETERMINES NaMBT INHIBITOR IN ETHYLENE GLYCOL-WATER SOLUTIONS

In studies of heat transfer media, problems of corrosion and the formation of insoluble residues have led to an improved method of quantitatively determining the sodium mercapto-benzothiazole (NaMBT) inhibitor in ethylene glycol-water solutions. The method is faster and more accurate than wet chemical techniques. It reduces analysis time, requires smaller samples, and detects extremely small concentrations of NaMBT.

Analyses are made using a spectrophotometer illuminated by light from a hydrogen source. Sample preparation depends upon the condition of the sample and the expected NaMBT concentration; samples which contain insoluble residues or which appear cloudy must be filtered before analysis. Also, because of the extreme sensitivity of the technique, the samples must be quantitatively diluted using distilled water (1:100).

The spectrophotometer is scanned from 360 to 200 nm, using a one-centimeter sample cell, with distilled water in the reference cell. The maximum absorption at 311 nm is compared to a previously prepared calibration curve to determine the amount of NaMBT present.

This technique has a detection limit of 250 ppm and is accurate to 0.005 percent.

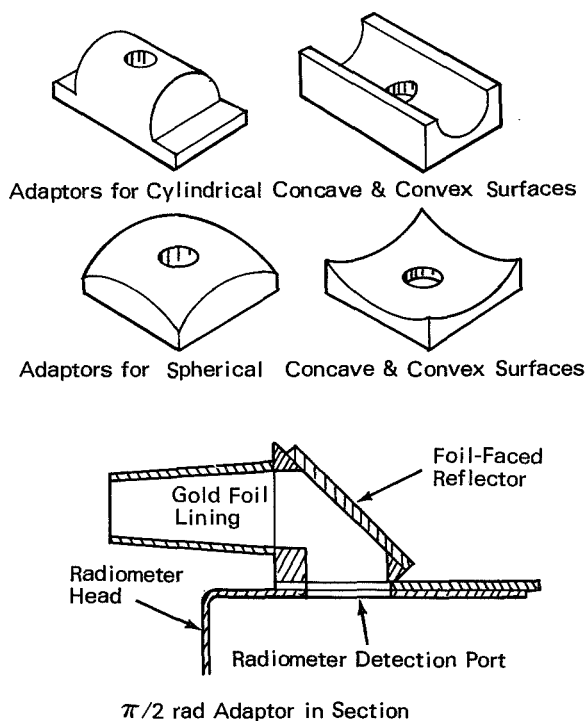
Source: G. G. Garrard of  
North American Rockwell, Inc.  
under contract to  
Manned Spacecraft Center  
(MSC-11496)

*Circle 18 on Reader Service Card.*

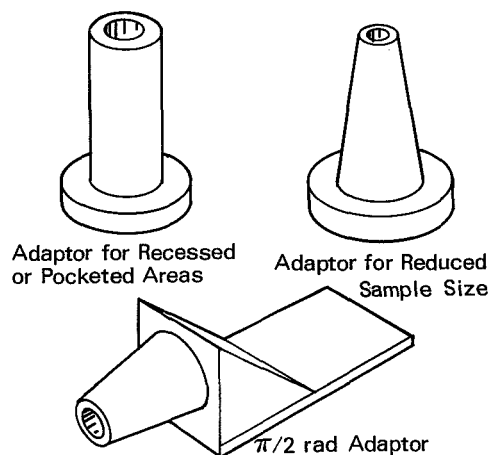
### REFLECTOMETER ADAPTORS

The capabilities of a conventional radiometer can be extended through the use of adaptors which permit measuring the surface emittance of items whose surface geometry does not conform

The adaptors, a number of which are shown in the illustration, have a front face shaped to permit complete contact with the surface to be measured, and a base which mates with the



to that of the radiometer. A typical radiometer head has a flat front surface approximately 15 cm in diameter, with a detection port 2.5 cm in diameter located off-center on its surface. The head carries its own source of infrared energy. Since the detection port must be placed flush against the sample surface in order to gather accurate reflectance data, various curved or recessed surfaces have been difficult to check.



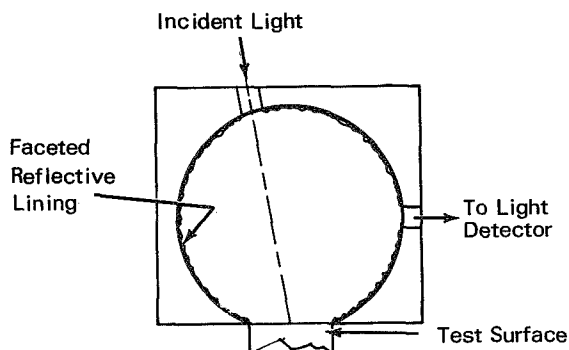
radiometer head. A hole bored straight through each adaptor and lined with gold (gold-coated tape) provides an efficient energy-transfer path to and from the radiometer head. A gold-foil-surfaced reflector is used whenever an angular adaptor is required. The gold coating, which has a reflectance of about 98% for infrared energy, guides the reflectometer's emission to the sample surface and the reflected energy back to the detector. Each adaptor is initially calibrated against a surface of known emissivity.

Source: B. Bandini of  
Grumman Aircraft Co.  
under contract to  
Manned Spacecraft Center  
(MSC-12338)

*Circle 19 on Reader Service Card.*

**INTEGRATING SPHERE OPERATES AT VISIBLE AND INFRARED WAVELENGTHS**

An optical integrating sphere with a faceted reflective lining on its inside surface provides light randomization (mixing of diffusely and



specularly reflected light) with relatively few reflections. The improved sphere has a sufficiently high reflectivity for both visible and infrared radiation that can be used for measuring the reflectivity of test surfaces over this spectral range. In the past, separate integrating spheres

were required for measurements in the visible and in the infrared regions.

The faceted lining can be formed in a number of ways. One involves folding and refolding aluminum foil to obtain the proper texture, and then shaping the foil to conform to the internal surface of the integrating sphere. Another method is to grind or machine and polish the facets on the outside of a sphere and then make a split mold of the faceted sphere using plastic casting or electroforming. The inside of the resulting faceted sphere can be made highly reflective by vacuum depositing a reflective metal or by applying a magnesium oxide coating.

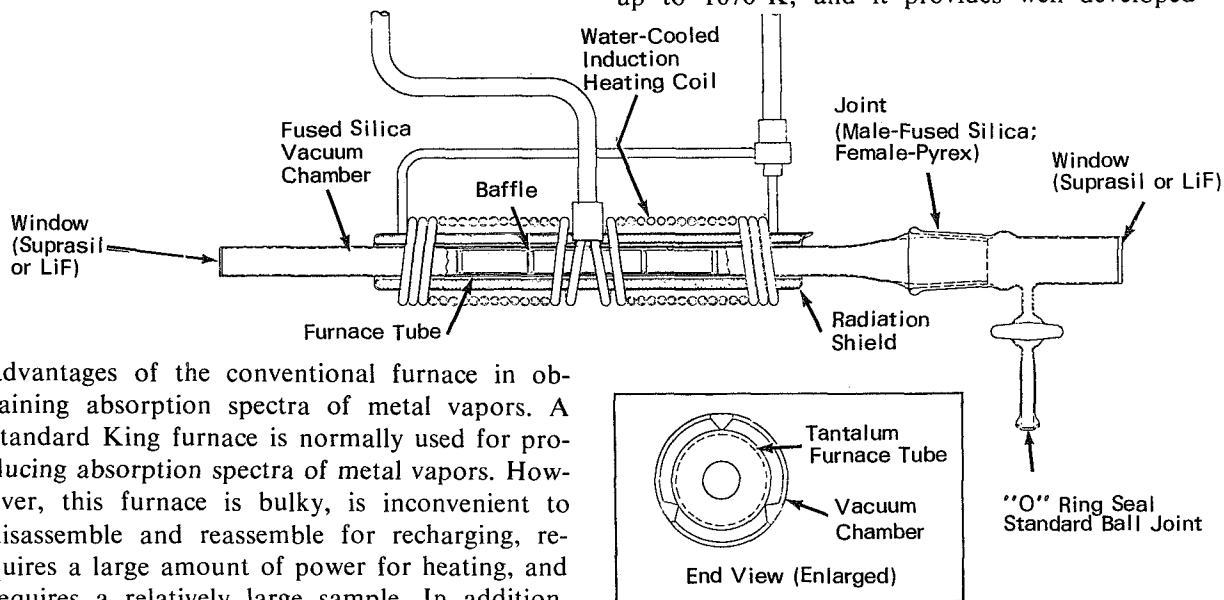
Source: S. Aisenberg of Space Sciences Inc. under contract to Marshall Space Flight Center (MFS-14248)

*Circle 20 on Reader Service Card.*

**MINIATURE KING FURNACE FOR SMALL-SAMPLE ABSORPTION SPECTROSCOPY**

A miniature King furnace, consisting of an inductively heated, small diameter tantalum tube supported in a radiation shield, eliminates the dis-

advantages of the conventional furnace in obtaining absorption spectra of metal vapors. A standard King furnace is normally used for producing absorption spectra of metal vapors. However, this furnace is bulky, is inconvenient to disassemble and reassemble for recharging, requires a large amount of power for heating, and requires a relatively large sample. In addition, there is the possibility of the sample reacting



with the furnace tube material to form carbides. The modified furnace is compact and easily assembled. It can be operated at temperatures up to 1670 K, and it provides well developed

absorption spectra with sample charges of only a few milligrams of metal.

The furnace apparatus, shown in the diagram, consists of four basic parts: the tantalum furnace tube, the vacuum chamber, the radiation shield, and the water-cooled, induction-heating coil. Four tantalum baffles are placed in the tube to inhibit diffusion of the sample during operation. Thermal contact between the furnace tube and the fused-silica vacuum chamber is minimized, permitting furnace operation at temperatures well above the softening temperature of quartz, without danger of vacuum chamber collapse. The radiation shield is a double-walled, fused-silica tube filled with finely divided carbon, outgassed and sealed off under vacuum.

The water-cooled induction heating coil is wound using standard copper tubing with hard-soldered joints. The center fed, parallel coil configuration minimizes high frequency excitation of the metal vapor or buffer gas in the furnace tube or vacuum chamber. The tank circuit of the induction heater oscillator is single ended. By applying the high potential to the center of the heating coil, discharge in the buffer gas or sample vapor is effectively eliminated.

Source: F. S. Tompkins and B. Ercoli  
Argonne National Laboratory  
(ARG-10177)

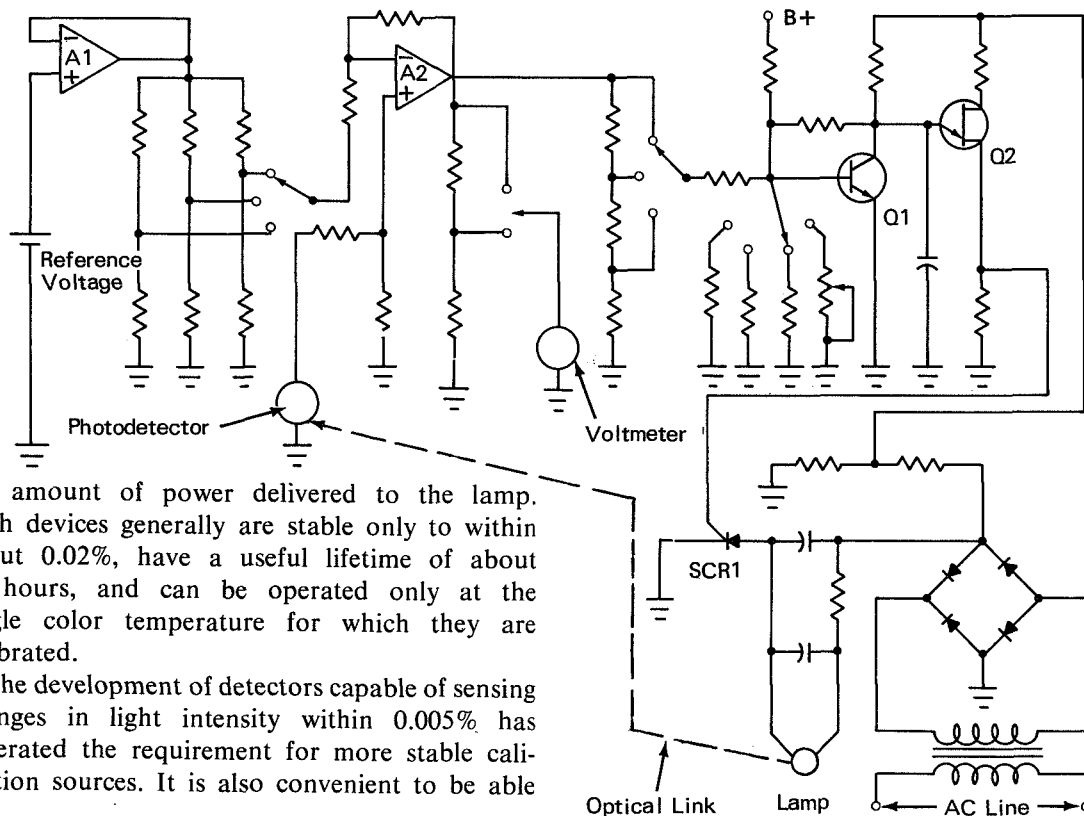
Circle 21 on Reader Service Card.

### CALIBRATED-INTENSITY LAMP

The illustration is a schematic diagram of the control circuitry for an ultrastable light source. Similar, commercially available devices use a current monitor to generate feedback and to control

to operate the source over a range of color temperatures.

In the ultrastable source illustrated, feedback is generated by a light-output monitor rather than



the amount of power delivered to the lamp. Such devices generally are stable only to within about 0.02%, have a useful lifetime of about 50 hours, and can be operated only at the single color temperature for which they are calibrated.

The development of detectors capable of sensing changes in light intensity within 0.005% has generated the requirement for more stable calibration sources. It is also convenient to be able

by a current monitor. This eliminates the effects of changing lamp filament resistivity or lamp envelope transparency. The circuit thus automatically compensates for aging, allowing a longer calibrated lifetime. The output stability is at least 0.005%, and the lamp may be calibrated and operated at several color temperatures.

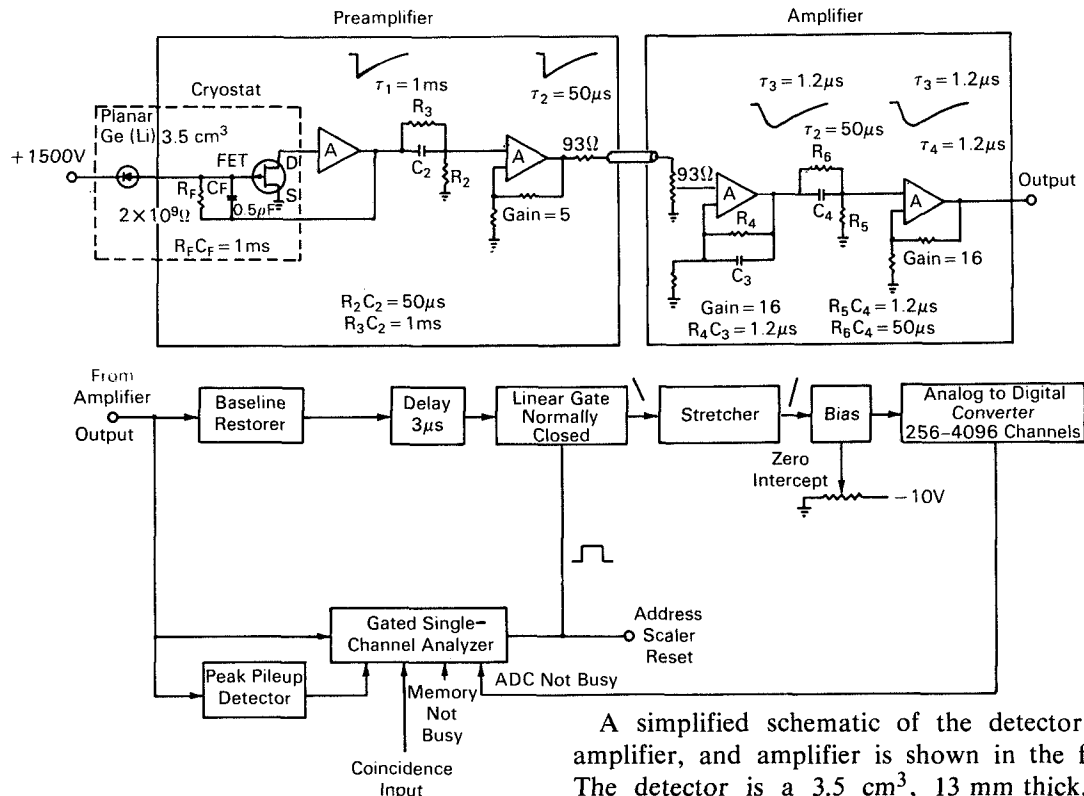
Source: M. F. Heidt and J. E. Novotny  
Manned Spacecraft Center  
and N. K. Shanker of  
Lockheed Electronics Co.  
under contract to  
Manned Spacecraft Center  
(MSC-12293)

Circle 22 on Reader Service Card.

### HIGH-RESOLUTION SPECTROMETER REDUCES RATE-DEPENDENT ERRORS AT HIGH COUNTING RATES

A modified spectrometer, incorporating a low-noise preamplifier, can be used to obtain good resolution at high counting rates in a Ge(Li) gamma-ray spectrometer. This preamplifier elim-

Pulse-shape and baseline discrimination are used to reject pileup pulses. The overall system resolution is nearly independent of rate for counting rates up to 25,000 counts/sec.



inates spectral distortions that occur in the conventional spectrometer at counting rates above a few thousand pulses/sec because of pulse undershoot, baseline shift, and pulse pileup.

In the modified unit, pole-zero cancellation is used to minimize pulse undershoots due to multiple time constants. Baseline restoration is used to improve resolution and prevent spectral shifts.

A simplified schematic of the detector, pre-amplifier, and amplifier is shown in the figure. The detector is a 3.5 cm<sup>3</sup>, 13 mm thick, lithium-drifted planar germanium diode, housed in a cryostat and cooled to 77 K. The pre-amplifier consists of two sections, a charge integrator and an output driver. The integrator input stage is a field effect transistor, direct-coupled to the detector and cooled to 77 K. The amplifier consists of two 3-transistor feedback loops with a gain of 16 dB per loop.

Pulses from the integrating section of the pre-amplifier are differentiated once in the pre-amplifier and again in the amplifier. To prevent undershoots due to multiple differentiation, pole-zero cancellation is used. To prevent rate effects and dc-level drift from affecting the baseline, a baseline restorer is used to superimpose each pulse on a stable dc level. The baseline restorer also acts as a nonlinear high-pass filter, thus improving the system signal-to-noise ratio.

Prior to encoding, a pulse is inspected for pileup. A baseline discriminator in the gated single-channel analyzer is triggered when an input pulse exceeds the noise level ( $\approx 50$  mV). Once triggered, the discriminator is held inoperative as long as the signal exceeds the noise level. The discriminator strobes an internal gate and, when all gating conditions are satisfied, a single-channel analyzer output is generated. If a second pulse occurs before the tail of the first pulse

has returned to within 50 mV of the baseline, the discriminator is not triggered. Thus, "tail pileup" pulses are rejected.

A pulse starting on the baseline may also have a pulse superimposed on its leading edge, causing distortion by "peak pileup". A peak pileup detector produces differentiated zero-crossing pulses. Since the zero-crossing of pileup pulses occurs later than that of undistorted pulses, the pileup pulses are readily gated out in the single-channel analyzer.

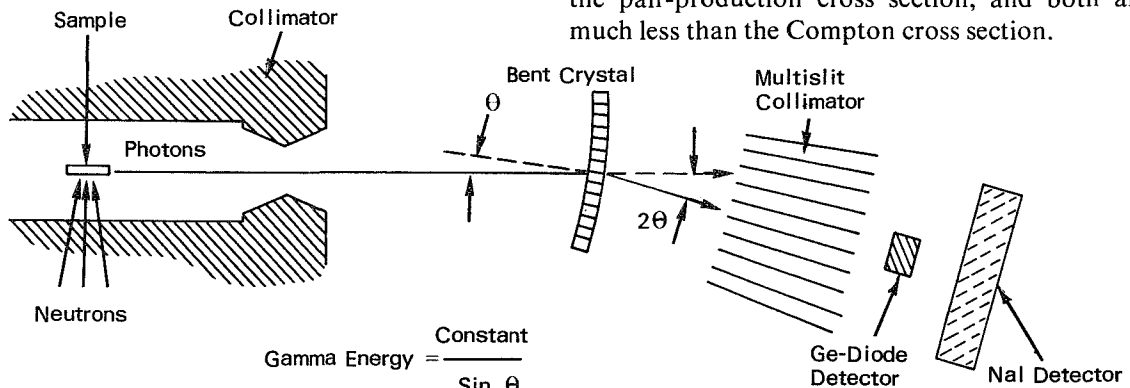
When an undistorted pulse is detected, the linear gate is opened. The selected pulse is then processed in the analog-to-digital converter and stored as digital data.

Source: M. G. Strauss, et. al., of  
Argonne National Laboratory  
(ARG-10144)

Circle 23 on Reader Service Card.

### HIGH-RESOLUTION GAMMA-RAY SPECTROMETER

A bent-crystal gamma-ray spectrometer combined with a lithium-drifted Ge-diode detector, performs high-resolution gamma-ray spectroscopy with significant improvements in resolution,



energy precision, and overall sensitivity. The system combines the energy precision of the bent-crystal spectrometer with the high resolution of the Ge-diode.

In performing high-resolution gamma-ray spectroscopy on complicated neutron-capture gamma-ray spectra, the most difficult region to analyze is the intermediate range (1-4 MeV). In this re-

gion, the  $(n, \gamma)$  spectrum is complex and the peak-to-background ratios are generally low. This is especially true in the 1-2 MeV range, where the photoelectric cross section is comparable to the pair-production cross section, and both are much less than the Compton cross section.

The new system, shown in the diagram, is most useful in the 1-3 MeV energy range, where its precision and energy resolution are from 3 to 10 times better than those of either the bent crystal or the Ge diode used individually, and the signal-to-background ratio is 50 times better.

The crystal diffraction process projects a limited energy region of the  $\gamma$  spectrum onto



the Ge-diode gamma detector. The high resolution of the diode then further resolves this narrow spectral region into its component parts.

There are three important facets in this process: (1) The gamma rays incident on the detector are limited to the small region under investigation, so that the total counting rate in the detector system can be kept low without losing sensitivity. This allows the use of an amplifier which has a slow response function and therefore the best possible energy resolution. (2) The large background of Compton events from the higher energy gammas in the full spectrum is eliminated, allowing a marked improvement in the peak-to-background ratio in the Ge detectors. (3) The relative intensity of the individual

components of the close doublet or complex structure can be controlled by adjusting the setting of the bent-crystal spectrometer. By recording a set of gamma-ray spectra taken with the Ge-diode detector at different settings of the bent-crystal spectrometer, additional information about the complex structure can be obtained. For example, one can enhance the weaker member of a close doublet. It is, in fact, this type of enhancement that leads to the energy-resolution improvement over what can be obtained with either system used individually.

Source: R. K. Smither and A. I. Namenson  
Argonne National Laboratory  
(ARG-10190)

*Circle 24 on Reader Service Card.*

### MULTICHANNEL SPECTROSCOPY GUIDE

A system of diverging duct walls is used in a spectrometer to conduct light from multiple entrance slits to multiple detectors. With this arrangement, shown in the illustration, the intensities of several closely-spaced narrow wave-

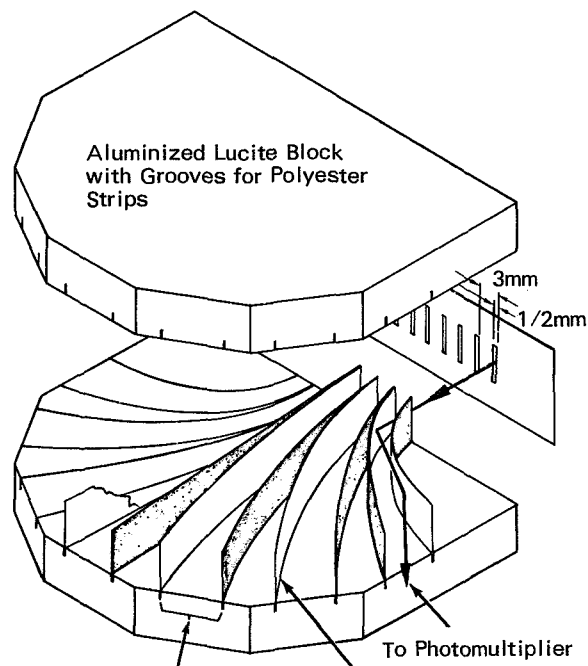
length areas in the light spectrum can be measured simultaneously. In cases such as shock-tube applications, which impose severe restrictions on the time available to obtain the data, it is not practical to scan the spectrum with a single photomultiplier. A separate detector must be used for each wavelength area to be investigated.

The ducts consist of polyester strips, aluminized on the inner sides to provide light paths with minimum absorption losses. The strips are mounted in matching, grooved, aluminized blocks that maintain proper duct alignment for optimum light delivery to the various photomultiplier tubes.

This duct arrangement is designed for the study of continuous spectra. The wavelength interval accepted by each channel can be changed by using different masks and different slit widths in the spectral plane. A variation for the simultaneous measurement of randomly displaced spectral-line intensities simply involves making each duct self-contained and movable.

Source: D. E. Rothe of  
Cornell Aeronautical Laboratory, Inc.  
under contract to  
NASA Headquarters  
(HQN-10441)

*Circle 25 on Reader Service Card.*



Light Channels Diverge  
for High Transmission  
Efficiency.

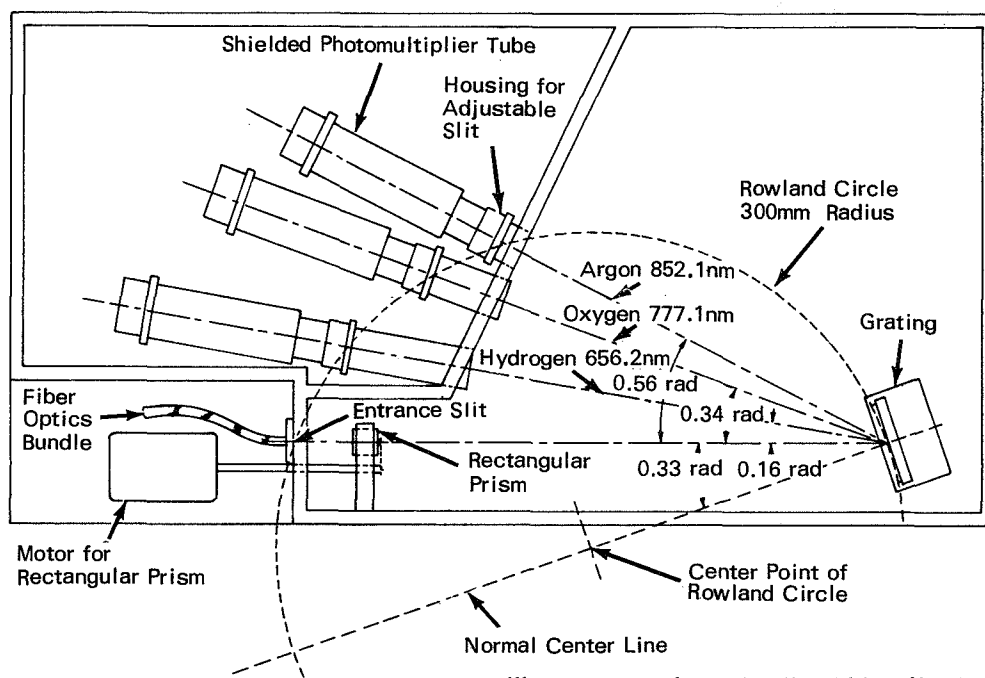
Polyester Strips  
Aluminized  
on One Side

## Section 3. Manufacturing and Quality Control Devices

### PORTABLE SPECTROMETER MONITORS INERT-GAS WELDING SHIELD

A spectrometer using photosensitive readouts can accurately monitor the amount of oxygen and hydrogen in the inert gas shield of a tungsten/inert-gas welding process.

The problem of blackbody radiation entering the spectrometer is eliminated by using an oscillating rectangular prism in the nondispersed light beam, causing the emission line to os-



The illustration shows the overall layout. The hydrogen 656.28 nm and oxygen 777.18 nm spectral lines are the analytical lines. The argon 852.14 nm line is the internal standard. These lines are chosen because there are no others closely adjacent to them.

Since the welding arc does not necessarily stay in a fixed plane, a fiber optic bundle is used to transmit the light from the arc to the spectrometer. One end of the bundle serves as the entrance slit, and the other as the limiting aperture. A 1 mm entrance slit is used to compensate in some degree for the light loss in the bundle; this wide an entrance slit is made possible by the lack of competing lines which otherwise would produce spectral interference.

cillate across the exit slit. This effectively produces an ac signal over the dc blackbody signal.

The solid-state readout system is a direct ratio system and is therefore very sensitive. Ratio computers are used in each channel to compare the analytical response readout with that of the internal standard. Outlets are also provided for oscilloscope monitoring of the waveform in order to establish proper optical alignment of the exit slits.

Source: E. L. Grove, et al., of  
IIT Research Institute  
under contract to  
Marshall Space Flight Center  
(MFS-12144)

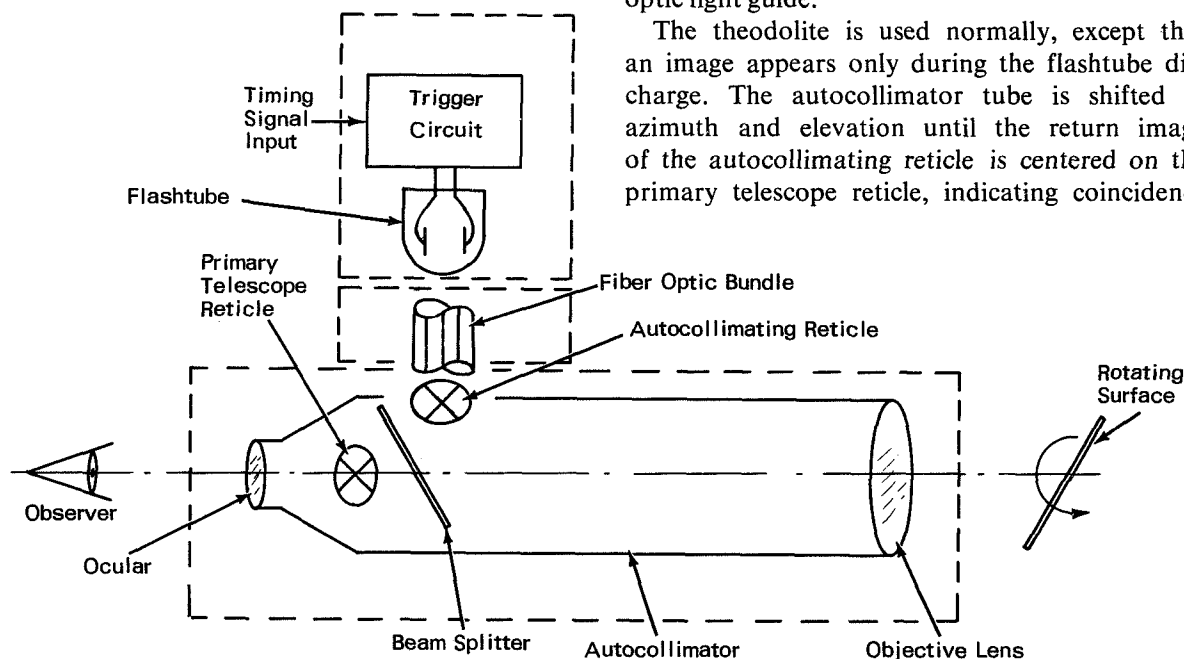
Circle 26 on Reader Service Card.

**STROBOSCOPIC AUTOCOLLIMATOR**

The purpose of the device shown in the illustration is to measure the instantaneous angle of a rotating surface in synchronism with an electrical timing signal supplied to the device. An

mounted in place of the usual autocollimating illuminator, or alternately, to keep the theodolite small and lightweight, the flashes may be optically coupled to the autocollimator by a fiber-optic light guide.

The theodolite is used normally, except that an image appears only during the flashtube discharge. The autocollimator tube is shifted in azimuth and elevation until the return image of the autocollimating reticle is centered on the primary telescope reticle, indicating coincidence



autocollimating theodolite is illuminated by a stroboscopic flashtube which generates optical pulses of 100 microseconds or less in duration. The flashtube is governed by an electronic triggering circuit, which in turn is activated by the electronic timing signal. The flashtube may be

between the autocollimator axis and the normal to the surface being measured.

Source: A. Jalink, Jr.,  
Langley Research Center  
(LAR-90292)

*No further documentation is available.*

**COORDINATE LOCATOR FOR PRINTED CIRCUIT BOARD HOLES: A CONCEPT**

A conceptual solution to the problem of accurately determining printed circuit board (PCB) template hole locations, in a desirable sequence, uses a fixed light source to register the X and Y coordinates in a fixed opaque template. Accurate hole positioning in the template is essential in using the template to make accurate, repeatable hole patterns in production circuit boards. The X-Y hole-coordinate information is used by numerically controlled drill presses, either directly or after reformatting by computer.

The concept involves using a parabolic mirror

and a set of photocells to detect the passage of light through the individual holes. A narrow slit is centrally located in the X direction on a smooth, opaque, stationary, primary surface, and runs completely across the surface in the Y direction. The light source is mounted above the slit, and the mirror is mounted directly below the slit, with its focal point located at the farthest point from the primary surface. A circuit board template is mounted beneath the primary surface on a table which is free to move from left to right.

As the template moves, light strikes the parabolic mirror each time a hole is traversed. The light is reflected to the mirror's focal point, where a photocell is located. The peak voltage output of the photocell locates the hole centerline in the X direction. With the template stationary, another photocell, equipped with a pinhole aperture and mounted in the narrow slit of the primary surface, moves from top to bottom in the slit. As it moves, light is received

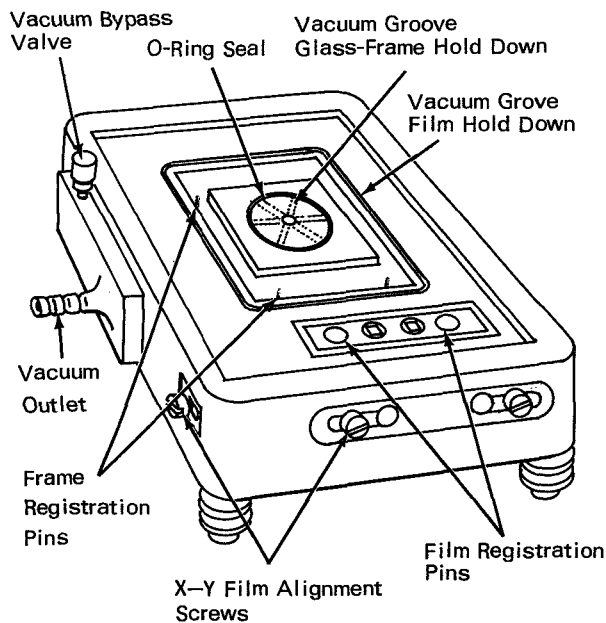
as soon as the leading edge of the hole is crossed and until the trailing edge is passed. In this case, the peak photocell output locates the Y coordinate of the hole centerline.

Source: L. W. Samuel of  
The Boeing Company  
under contract to  
Marshall Space Flight Center  
(MFS-14737)

Circle 27 on Reader Service Card.

### PRECISION ALIGNMENT FIXTURE FOR PRODUCING PHOTO-RESIST ETCHED WAFERS

The device shown in the illustration exposes photo-resist emulsion through a negative mask, and has an overall registration accuracy of  $\pm 0.0013$  cm.



The procedure involving the fixture is as follows: A negative mask (film photomaster) is optically aligned and precision punched to a master

set of fiducial marks. A photo-resist coated metal-glass-frame assembly is placed into the alignment fixture. The slide assembly is positioned against the three frame-registration pins. A vacuum is applied to hold the slide assembly securely in place. The punched film is placed on the alignment pins of the registration fixture. Vacuum is applied through the bypass valve to the film hold-down grooves, pulling the film (emulsion down) into intimate contact with the photo-resist coating. Ultraviolet light is applied from an overhead source into the top of the alignment fixture. The light passes through the clear areas of the film negative into the photo-resist coating on the slide assembly. The photo-resist emulsion with the image permanently recorded in its molecular structure, is developed and etched to produce the final registered image in the alum coating.

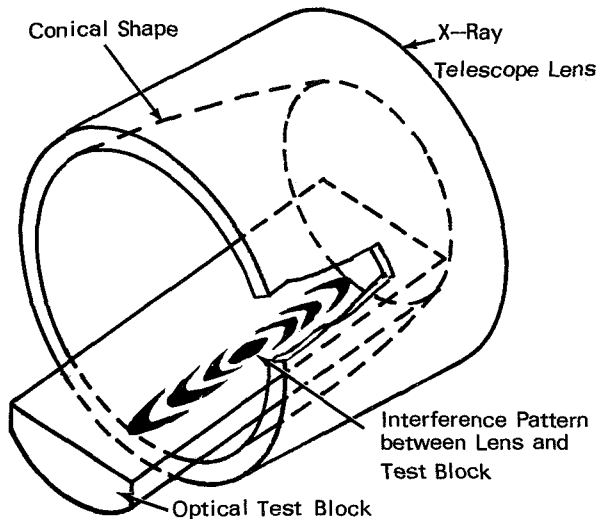
Source: E. S. Sweningson and R. D. Hilgeman of  
Philco Corp.  
under contract to  
Manned Spacecraft Center  
(MSC-12063)

No further documentation is available.

### FORM GAGE FOR CONICAL OPTICAL SURFACE

The device shown in the illustration is used to measure form and smoothness during the finishing of the reflecting lenses for an X-ray

telescope. A test block, in the form of a segment of an optical cylinder with a radius slightly smaller than that of the lens to be

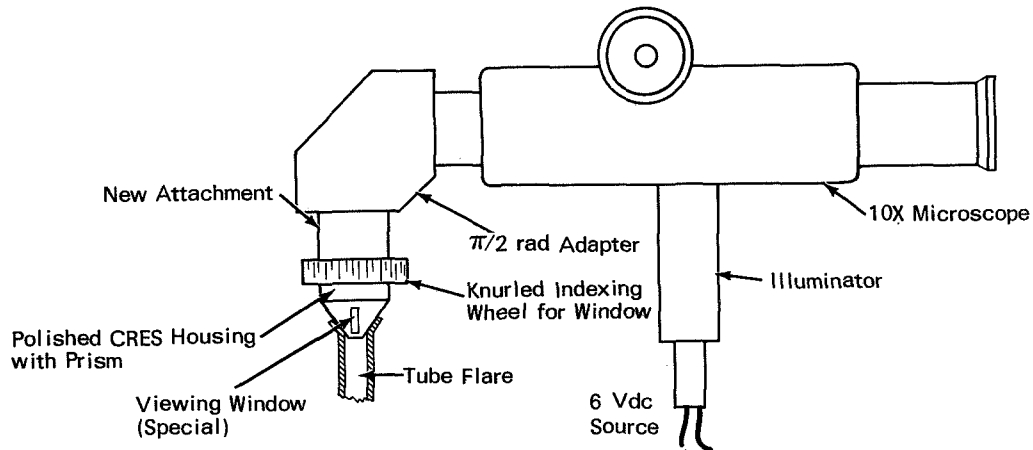


measured, is inserted into the lens and placed in close proximity to the reflecting surface of the lens. When the system is illuminated with monochromatic light, an interference pattern (Newton's rings) is formed. The pattern is photographed and the fringe positions are translated into the actual form of the mirror surface. With care, the location of fringes in the pattern can be measured to within about 0.1 fringe. This translates into a measurement accuracy of about  $\pm 2$  nm on the optical surface.

Source: W. Angele  
Marshall Space Flight Center  
(MFS-20124)

Circle 28 on Reader Service Card.

**MAGNIFIER FOR IN-PLACE INSPECTION OF TUBE FLARES**



A special adapter, containing a rotatable prism and a cone-angle viewing window attached to a commercial ten-power illuminated microscope and right-angle adapter, permits in-place inspection of tube flares after assembly. As shown in the illustration, the viewing window can be inserted into the flare cone after disconnecting the attached line and slightly displacing the flared

end. By rotating the viewing window, the entire surface of the flare can be inspected.

Source: R. E. Rush of  
North American Rockwell, Inc.  
under contract to  
Manned Spacecraft Center  
(MSC-15349)

No further documentation is available.

### OPTICAL TEMPLATE MEASURES VERY SMALL CORNER RADII

An optical template with a magnifier can be used to measure very small corner radii where an optical comparator cannot be used, and where limited accuracy is acceptable. The photoetched template should contain a set of graded-size circles, calibrated according to the power of the magnifier. A pair of perpendicular tangent lines may be added to each circle to aid in aligning a circle with the corner to be measured. The unit's small size and portability make it

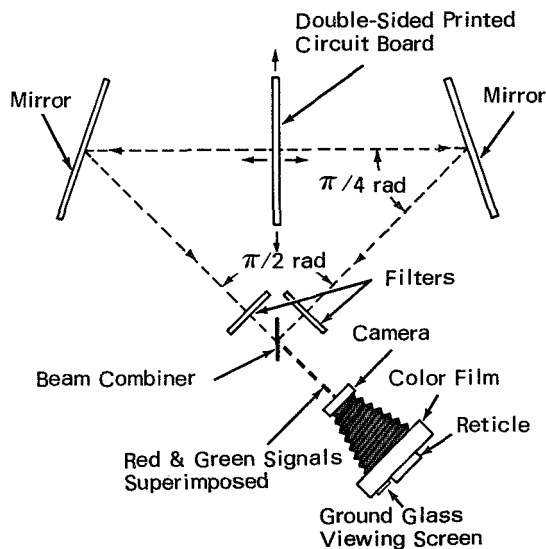
especially useful for examining, comparing, and checking the tolerance of very small holes, fillets, and chamfers.

Source: K. Loo of  
North American Rockwell, Inc.  
under contract to  
Marshall Space Flight Center  
(MFS-91458)

*No further documentation is available.*

### CAMERA SYSTEM FOR PRINTED CIRCUIT BOARD INSPECTION

An optical comparator, in which color-coded images of both sides of a printed circuit board (PCB) are superimposed, provides a means for



accurately determining the quality and registration of surface features of double-sided PCB's. Present PCB visual inspection methods using magnifiers and a reticle are slow and tedious.

As shown in the illustration, the method employs two light sources, arranged to illuminate

each side of the PCB. Surface features of the circuitry are reflected by the two mirrors through primary color filters (for example, red and green). The color-coded images are superimposed by the beam combiner (a half-surfaced mirror) before passing into the camera lens. In the camera, the superimposed images are focused onto a ground glass screen, either in true size or under magnification.

A calibrated reticle capable of various magnifications can be used to measure image details. The superimposed images can also be photographed on either color or high-resolution black and white film to provide a permanent record. The superimposition immediately reveals deviations from proper registration, as well as surface details of each side of the PCB. The screen displays a dominant color mixture for features in registration and a discrete primary color (depending on the two filters used) for features which are not in precise registration.

Source: M. Cridlin and J. O'Connor  
Goddard Space Flight Center  
(GSC-07971)

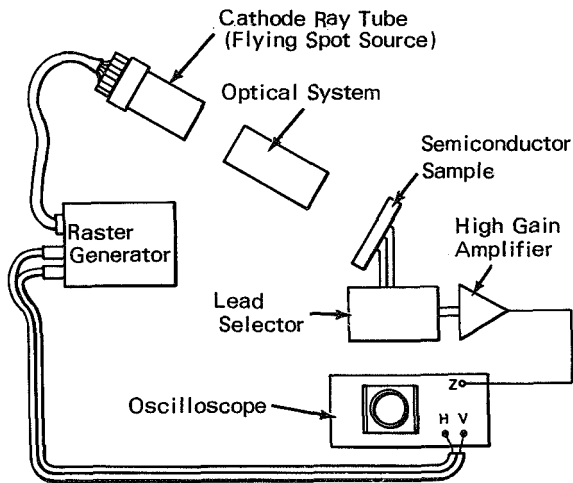
*Circle 29 on Reader Service Card.*

### DEVICE VISUALLY PORTRAYS SEMICONDUCTOR SURFACES

A device based on the principle that the surface layers of a semiconductor will conduct an electric current when exposed to a beam of

light provides a visual representation of the physiochemical condition of the semiconductor surface layers.

The apparatus shown in the diagram consists of:



television set; an optical system; a lead selector that provides an electrical path between any two electrodes positioned on the surface of the semiconductor; a high-gain amplifier; and an oscilloscope. The horizontal and vertical sweep

voltages of the oscilloscope are synchronized with those of the raster generator, and the output voltage from the amplifier is fed to the Z-axis (intensity modulation) input of the oscilloscope.

As the light beam from the optical system scans the semiconductor surface, the instantaneous current between pairs of selected electrodes connected to the semiconductor varies in accordance with the characteristics of the surface between the electrodes. The light intensity variations in the pattern on the oscilloscope correspond to the current variations and permit analysis of the semiconductor surface layer characteristics with respect to the inversion layer, diffusion voids and excesses, crystal imperfections, and masking problems.

Source: R. A. Summers of Jet Propulsion Laboratory under contract to NASA Pasadena Office (JPL-00665)

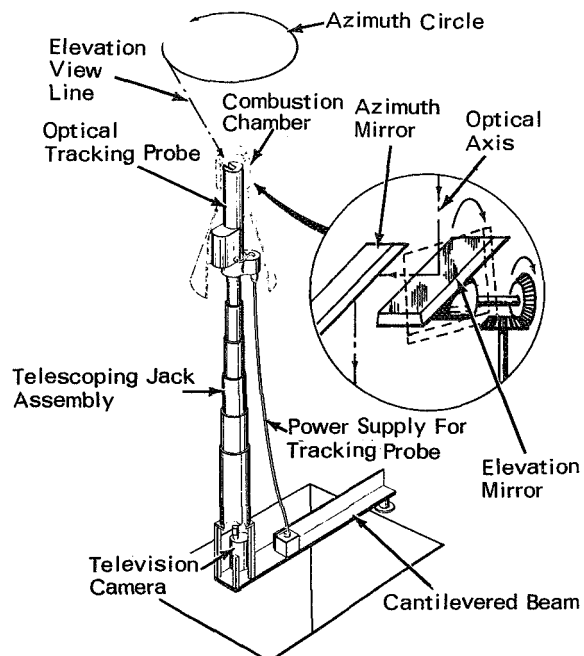
Circle 30 on Reader Service Card.

### IMPROVED OPTICAL PROBE FOR COMBUSTION CHAMBERS

A new probe permits remote inspection of combustion chambers throughout a field of view of almost  $4\pi$  steradians, and is fully controllable in terms of elevation, focus, and sweep. The device is a significant improvement over existing probes, which are quite limited in their field of view.

A perspective view of the probe is shown in the figure. The apparatus consists of an optical tracking probe mounted on a telescoping jack assembly. The probe and jack assembly are mounted on a cantilevered beam for positioning the probe directly under the combustion chamber. Operation of the jack raises the probe into the combustion chamber. The top portion of the probe may be equipped with lights, which may in turn be enclosed in an explosion-proof housing to eliminate any fire hazard. The apparatus also includes a television camera focused to receive the image transmitted by the probe.

Details of the optical tracking probe mirror



assembly are shown in the inset figure. The azimuth and elevation mirrors, as well as the focusing of an objective lens (not shown), are remotely controlled by three motors. The elevation mirror rotates about an axis perpendicular to the optical axis of the probe. The mirror is inclined to this axis by about  $\pi/4$  rad ( $45^\circ$ ), enabling it to sweep a vertical sector (longitude) of the spherical field of view as it rotates.

The azimuth mirror is rigidly attached to the

body of the probe, with an inclination of  $\pi/4$  rad to the optical axis. This allows the mirror to sweep a horizontal sector (latitude) of the spherical field of view as the probe body is rotated.

Source: J. Walker of  
Ling Temco Vaught  
under contract to  
Manned Spacecraft Center  
(MSC-10953)

*Circle 31 on Reader Service Card.*

---



NATIONAL AERONAUTICS AND SPACE ADMINISTRATION

WASHINGTON, D. C. 20546

OFFICIAL BUSINESS

PENALTY FOR PRIVATE USE \$300

FIRST CLASS MAIL



POSTAGE AND FEES PAID  
NATIONAL AERONAUTICS AND  
SPACE ADMINISTRATION

POSTMASTER: If Undeliverable (Section 158  
Postal Manual) Do Not Return

*"The aeronautical and space activities of the United States shall be conducted so as to contribute . . . to the expansion of human knowledge of phenomena in the atmosphere and space. The Administration shall provide for the widest practicable and appropriate dissemination of information concerning its activities and the results thereof."*

— NATIONAL AERONAUTICS AND SPACE ACT OF 1958

## NASA TECHNOLOGY UTILIZATION PUBLICATIONS

These describe science or technology derived from NASA's activities that may be of particular interest in commercial and other non-aerospace applications. Publications include:

**TECH BRIEFS:** Single-page descriptions of individual innovations, devices, methods, or concepts.

**TECHNOLOGY SURVEYS:** Selected surveys of NASA contributions to entire areas of technology.

**OTHER TU PUBLICATIONS:** These include handbooks, reports, conference proceedings, special studies, and selected bibliographies.

Technology Utilization publications are part of NASA's formal series of scientific and technical publications. Others include Technical Reports, Technical Notes, Technical Memorandums, Contractor Reports, Technical Translations, and Special Publications.

*Details on their availability may be obtained from:*

*Details on the availability of these publications may be obtained from:*

National Aeronautics and  
Space Administration  
Code KT  
Washington, D.C. 20546

National Aeronautics and  
Space Administration  
Code KS  
Washington, D.C. 20546

NATIONAL AERONAUTICS AND SPACE ADMINISTRATION

Washington, D.C. 20546